Electronic Supplementary Material (ESI) for Polymer Chemistry.
This journal is © The Royal Society of Chemistry 2023

# Exploring telogen chemical structure and reactivity when forming highly branched polyesters derived from ethylene glycol dimethacrylate homopolymerisation under Transfer-dominated Branching Radical Telomerisation (TBRT) conditions

Sean Flynn,[a,b] Bethany Linthwaite,[a,b] Oliver B. Penrhyn-Lowe,[a,b] Samuel Mckeating,[a,b] Stephen Wright,[a,b] Savannah R. Cassin,[a,b] Pierre Chambon,[a,b] and Steve P. Rannard*[a,b]

[a] Materials Innovation Factory, University of Liverpool, 51 Oxford Street, Liverpool, L7 3NY, UK

[b] Department of Chemistry, University of Liverpool, Crown Street, Liverpool, L69 7ZD, UK

[*] Corresponding author: E-mail: srannard@liv.ac.uk

## Experimental

### Materials

Anisole (>99%), 2,2′-azobis(2-methylpropionitrile) (AIBN, 98%), benzyl mercaptan (BzM, 99%), chloroform-*d* ($CDCl_3$, 99.8%D), cyclohexane thiol (CHT, 97%), ethylene glycol methacrylate (EGDMA, 98%), methyl methacrylate (MMA, 99%), phenylethyl mercaptan (PhEM, >99%), 4-*tert*-butyl benzyl mercaptan (*t*BBM) were purchased from Sigma Aldrich. Ethyl acetate (EtOAc, analytical grade), methanol (MeOH, analytical grade) and tetrahydrofuran (THF, HPLC-grade) were purchased from Fischer. All materials were used as received.

### Methods

*Nuclear magnetic resonance spectroscopy (NMR)*

$^1H$ and $^{13}C$ NMR spectra were recorded on a Bruker Advance DPX-400 MHz spectrometer; $^1H$ and $^{13}C$ spectra were recorded at a frequency of 400 and 100 MHz respectively. Samples were analysed in deuterated chloroform ($CDCl_3$) at ambient temperature. Chemical shifts (δ) are reported in parts per million (ppm) relative to the known solvent chemical shift (δ = 7.26 ppm).

*Size-exclusion chromatography (SEC)*

Triple-detection SEC (TD-SEC) of branched polymers was performed using a Malvern Viscotek instrument, equipped with a GPCmax VE2001 auto-sampler, two Viscotek T6000M columns (and a guard column) and a triple detector array TDA305 containing a refractive index (RI) detector VE3580 and a 270 Dual Detector (light scattering and viscometer). A mobile phase of THF at 35 °C was used at a flow-rate of 1 mL $min^{-1}$. All samples were dissolved in the eluent at concentrations ≤5 mg $mL^{-1}$ and filtered through a 0.2 μm PTFE syringe filter prior to injection. Narrow and broad polystyrene standards (Viscotek, $M_w$ = 105 kg $mol^{-1}$, Đ = 1.02 and $M_w$ = 245 kg $mol^{-1}$, Đ = 2.27 respectively) were used as calibrants. SEC analysis of linear telomers was performed using a Malvern Viscotek instrument, equipped with a GPCmax VE2001 auto-sampler, a mixed column setup of one T2000 column and one T1000 column in series (and a guard column). A mobile phase of THF at 35 °C was used at a flow-rate of 1 mL $min^{-1}$. Samples were dissolved in the eluent at concentrations ≤10 mg $mL^{-1}$ and filtered through a 0.2 μm PTFE syringe filter prior to injection. All TD-SEC associated data were estimated using Omnisec software (Version 5.1).

*Matrix-assisted laser desorption ionisation – time of flight (MALDI-TOF) mass spectrometry*

MALDI-TOF analysis of linear telomers were analysed using a Bruker Autoflex Mass Spectrometer (Materials Innovation Factory, Liverpool, UK). Spectra obtained for linear telomers were each the sum of 500 shots acquired in positive-reflectron mode. Cesium triiodide (CsI3) and α-cyano-4-hyrdroxycinnamic acid (HCCA) were used as the mass scale calibrant and matrix, respectively. Both the matrix and samples were prepared at 10 mg $mL^{-1}$ in THF. The solutions were combined at a 5:1 v/v ratio of matrix to sample. 2 μL of the prepared solutions were deposited onto stainless-steel sample plates and air dried prior to analysis.

*Gas Chromatography (GC)*

GC was conducted using a HP-689 gas chromatography instrument equipped with a HP-5 column (30m × 0.54 mm × 0.5 mm); anisole was used as the internal standard. The carrier gas was hydrogen at 1 mL

$min^{-1}$. The column temperature was increased from a starting value of 90 °C to a maximum of 300 °C at a rate of 10 °C $min^{-1}$. Peaks were identified based on the corresponding pure reactants. Conversions were calculated based on changes in peak intensities relative to those obtained for an internal standard.

*General procedure for TBRT of EGDMA*

In a typical TBRT of EGDMA and *t*BBM, EGDMA (3.00 g, 15.1 mmol, 0.85 equiv.), *t*BBM (3.21 g, 17.8 mmol, 1.00 equiv.) and AIBN (0.0746 g, 0.454 mmol) were placed into a 25 mL round-bottom flask equipped with a magnetic stirrer bar. Ethyl acetate (6.60 g, 7.32 mL) was added and the solution was deoxygenated using a nitrogen purge under magnetic stirring for 30 minutes. An aliquot (~100 μL) of the mixture was taken for determination of the molar ratio of EGDMA to *t*BBM prior to initiation ($[EGDMA]_0/[Tel]_0$) by $^1H$ NMR analysis. The flask was then placed in an oil bath at 70 °C for 24 hours. The reaction was stopped *via* cooling and exposure to air. An aliquot (~100 μL) of the reaction mixture was taken for determination of vinyl conversion by $^1H$ NMR spectroscopy. The reaction mixture was then diluted in THF and precipitated into methanol (using a good solvent: anti-solvent volume ratio of 1:20) at ambient temperature, yielding a white precipitate. The polymer was dried *in vacuo* at 40 °C overnight to yield *p*(*t*BBM-EGDMA) as a white powder. The product was analysed by TD-SEC and both $^1H$ and $^{13}C$ NMR spectroscopy. All reactions were conducted using a fixed mass of ethyl acetate to ensure a constant concentration of EGDMA during TBRT.

*General procedure for linear telomerisation of MMA*

In a typical linear telomerisation of MMA and *t*BBM, MMA (1.00 g, 9.99 mmol, 5 equiv.), *t*BBM (0.361 g, 2.00 mmol, 1.00 equiv.) and AIBN (0.0246 g, 0.150 mmol) were placed into a 10 mL round-bottom flask equipped with a magnetic stirrer bar. Ethyl acetate (1.41 g, 1.56 mL) was added and the solution was deoxygenated using a nitrogen purge under magnetic stirring for 30 minutes. An aliquot (~100 μL) of the mixture was taken for determination of the molar ratio of MMA to *t*BBM prior to initiation ($[MMA]_0/[Tel]_0$) by $^1H$ NMR analysis. The flask was then placed in an oil bath at 70 °C for 24 hours. The reaction was stopped *via* cooling and exposure to air. An aliquot (~100 μL) of the reaction mixture was taken for determination of MMA conversion by $^1H$ NMR spectroscopy. The crude samples were concentrated *in vacuo* initially using a spiral evaporator and finally a vacuum oven at 40 °C for 24 hours. The crude product was then analysed by SEC and MALDI-TOF spectrometry.

*General procedure for kinetic monitoring of TBRT*

TBRT kinetic studies were conducted in a near-identical manner to the 'General procedure for TBRT of EGDMA' described above; however, 0.500 g of the EtOAc solvent system was replaced with anisole (0.500 g, 0.503 mL) in order to provide an internal standard for determination of EGDMA and telogen conversions by GC analysis. Kinetic studies were conducted using the highest common molar ratio of EGDMA to telogen at which all telogens produce soluble branched polymers under these conditions ($[EGDMA]_0/[Tel]_0 = 0.45$). Aliquots (*ca.* 200 μL) were taken from reaction mixtures at predetermined time intervals and were placed in a cooled glass vial containing BHT (*ca.* 1 mg) and were rapidly diluted with the corresponding cold analytical solvent (EtOAc and $CDCl_3$ for GC and $^1H$ NMR spectroscopy respectively). EGDMA and telogen conversions were determined by GC analysis and total vinyl conversion was determined by $^1H$ NMR spectroscopy.

*Differential scanning calorimetry (DSC)*

Thermal analyses were conducted using a TA Instruments Discovery DSC 25 instrument equipped with a RCS90 cooling unit. The following thermal protocol was used for all DSC analyses: (1) the sample was heated to 200 °C and subjected to a 3-minute isotherm to erase its thermal history, (2) the sample was then cooled to -90 °C at a rate of -10 °C $min^{-1}$ followed by a 30-minute isotherm. (3) glass transitions were then studied during heating of the sample to 150 °C at a rate of 20 °C $min^{-1}$. Glass transition temperatures ($T_g$) were recorded using TA Instruments software, TRIOS.

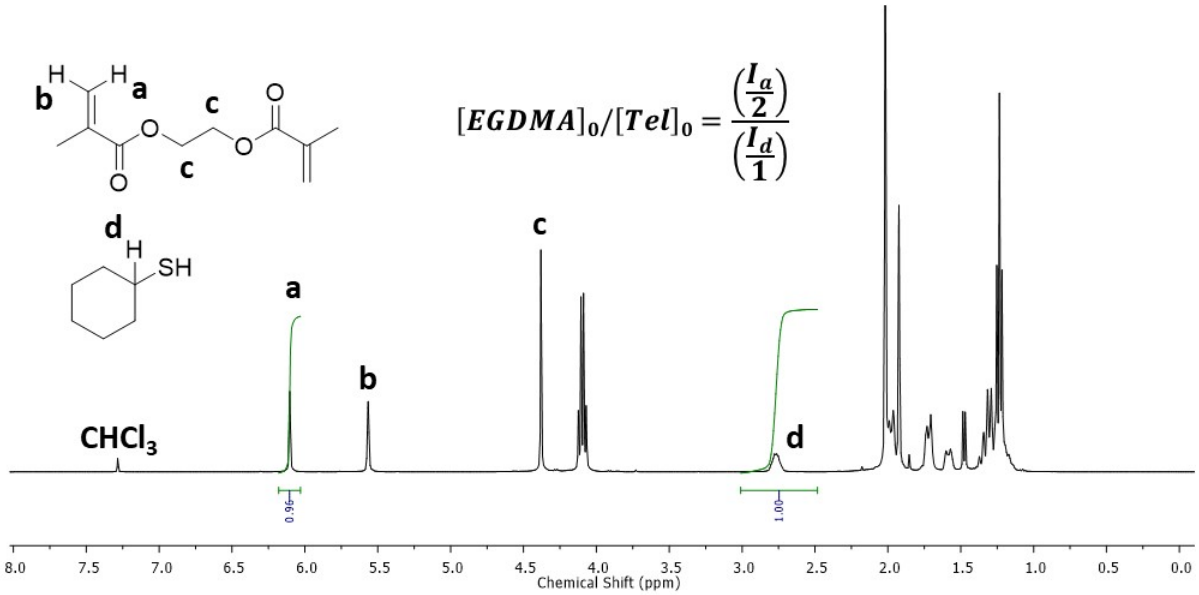


**Figure S1** $^1$H NMR (400 MHz, $CDCl_3$) spectrum obtained from TBRT of EGDMA with CHT prior to thermal initiation ($t_0$). The equation provided was used to determine the initial ratio of EGDMA to CHT ($[EGDMA]_0/[Tel]_0$).

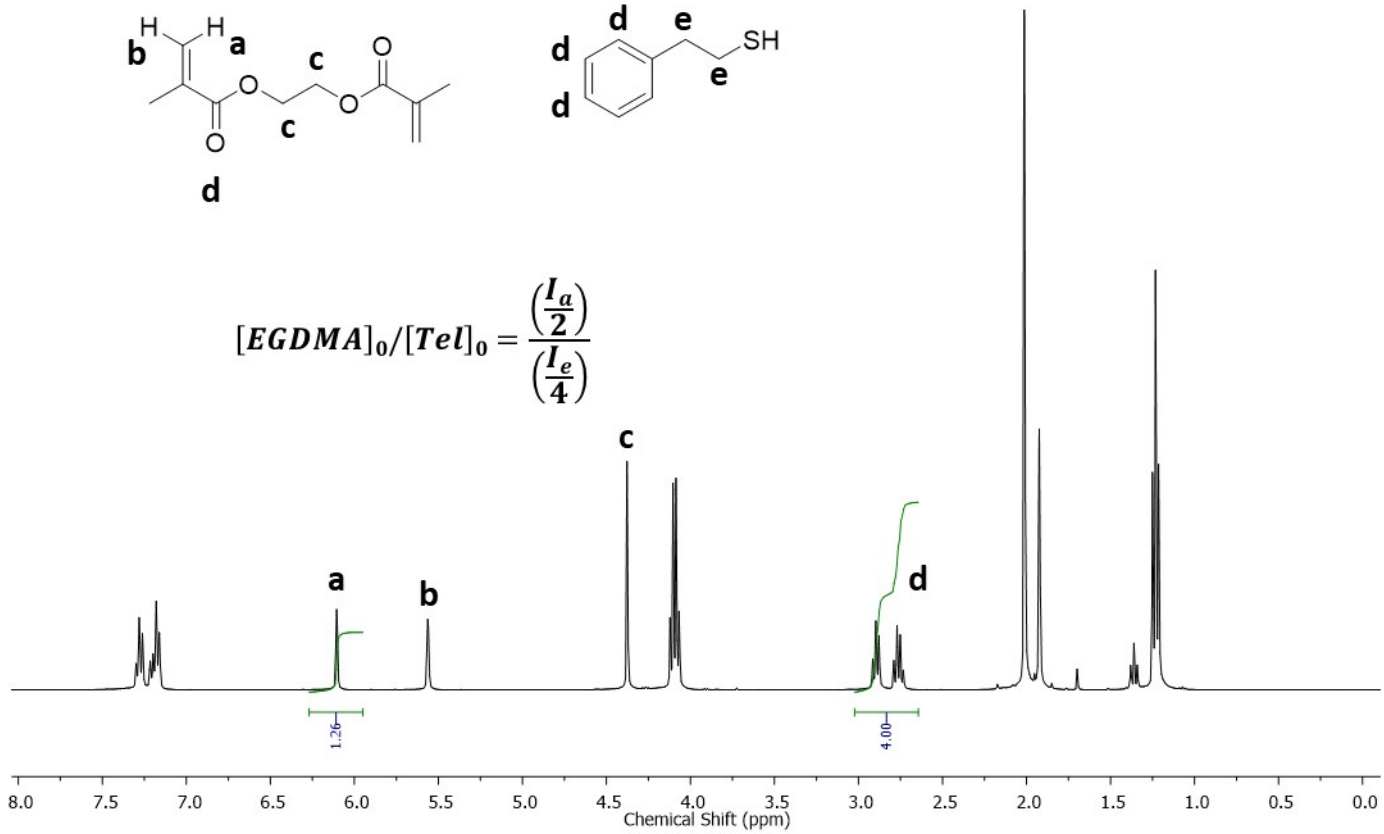

**Figure S2** $^1$H NMR (400 MHz, $CDCl_3$) spectrum obtained from TBRT of EGDMA with PhEM prior to thermal initiation ($t_0$). The equation provided was used to determine the initial ratio of EGDMA to PhEM ($[EGDMA]_0/[Tel]_0$).

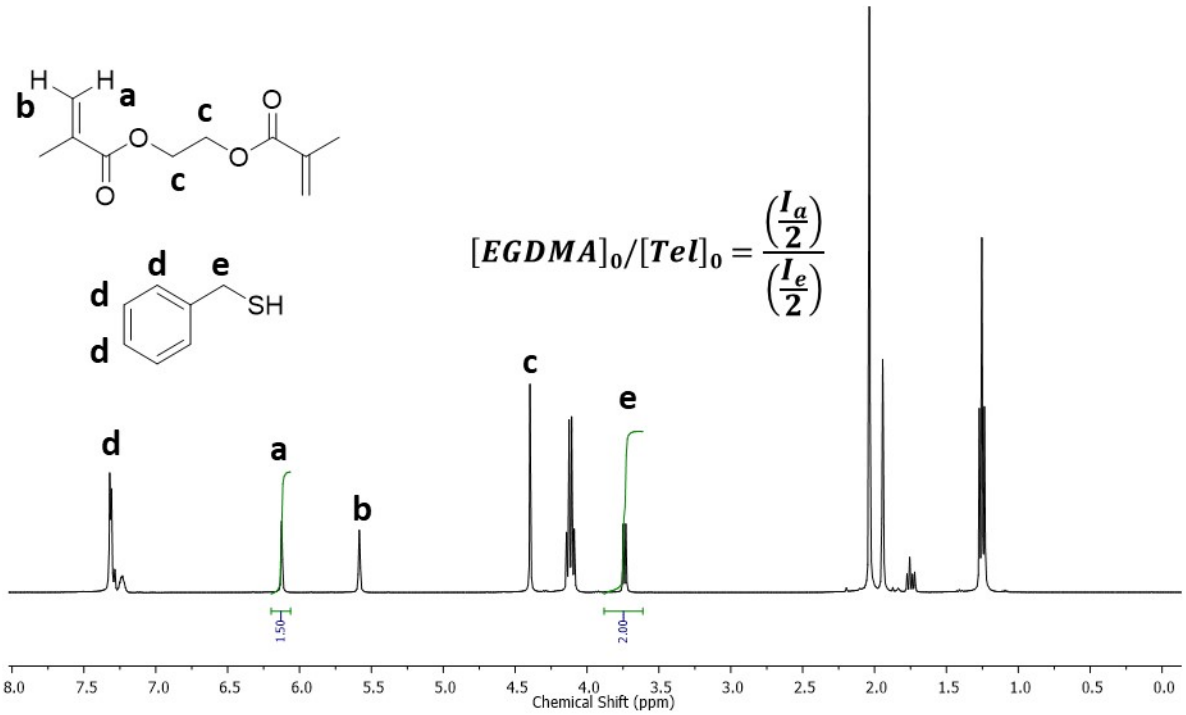


**Figure S3** $^1$H NMR (400 MHz, $CDCl_3$) spectrum obtained from TBRT of EGDMA with BzM prior to thermal initiation ($t_0$). The equation provided was used to determine the initial ratio of EGDMA to BzM ($[EGDMA]_0/[Tel]_0$).

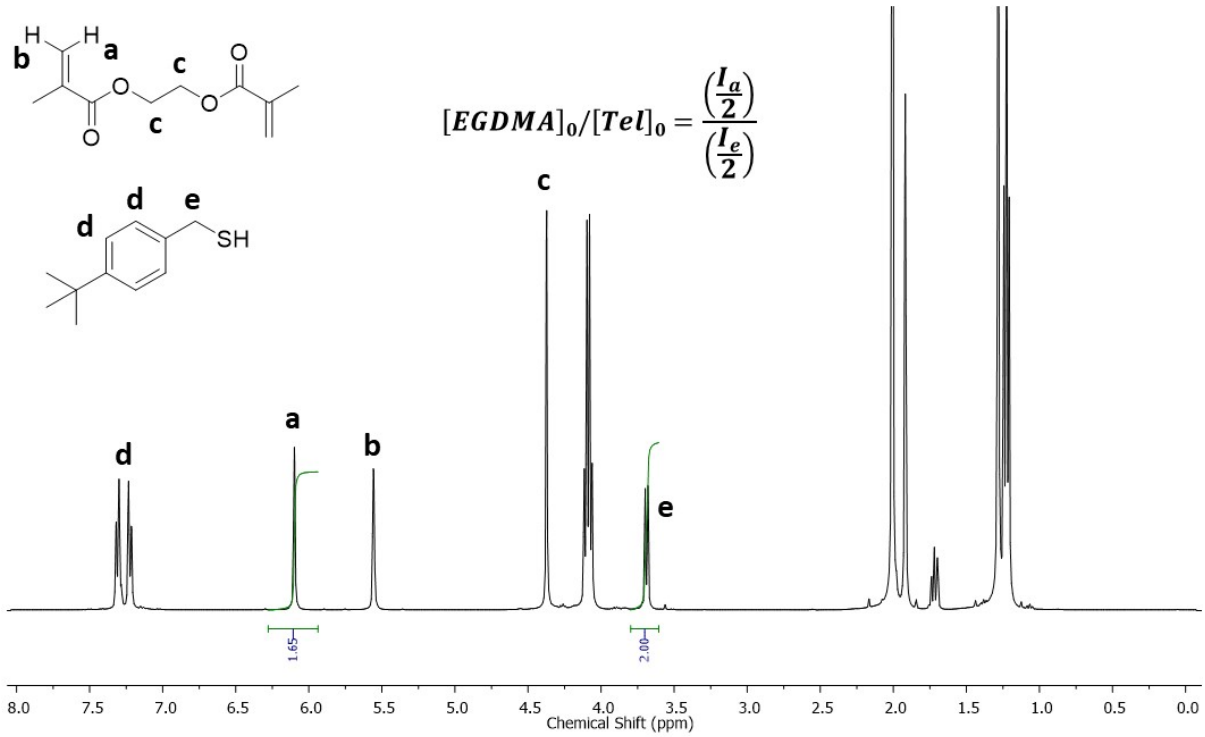

**Figure S4** $^1$H NMR (400 MHz, $CDCl_3$) spectrum obtained from TBRT of EGDMA with *t*BBM prior to thermal initiation ($t_0$). The equation provided was used to determine the initial ratio of EGDMA to *t*BBM ($[EGDMA]_0/[Tel]_0$).

**Table S1** $^1$H NMR spectroscopic and TD-SEC characterisation of branched polyesters prepared by TBRT of EGDMA with CHT, PhEM, BzM and tBBM.

| Telogen | $^1$H NMR ($CDCl_3$) | | | TD-SEC (THF) | | | |
|---|---|---|---|---|---|---|---|
| | $[EGDMA_0]/[Tel]_0$ | Vinyl conv. (%) | $[EGDMA]_F/[Tel.]_F$ | $M_w$ (g mol$^{-1}$) | $M_n$ (g mol$^{-1}$) | Đ | α |
| CHT | 0.45 | >99 | 1.02 | 328731 | 14602 | 154.23 | 0.325 |
| PhEM | 0.45 | >99 | 1.00 | 52014 | 5540 | 9.39 | 0.325 |
| BzM | 0.45 | >99 | 1.02 | 14748 | 4075 | 3.62 | 0.320 |
| *t*BBM | 0.45 | >99 | 1.01 | 9007 | 1336 | 6.74 | 0.269 |

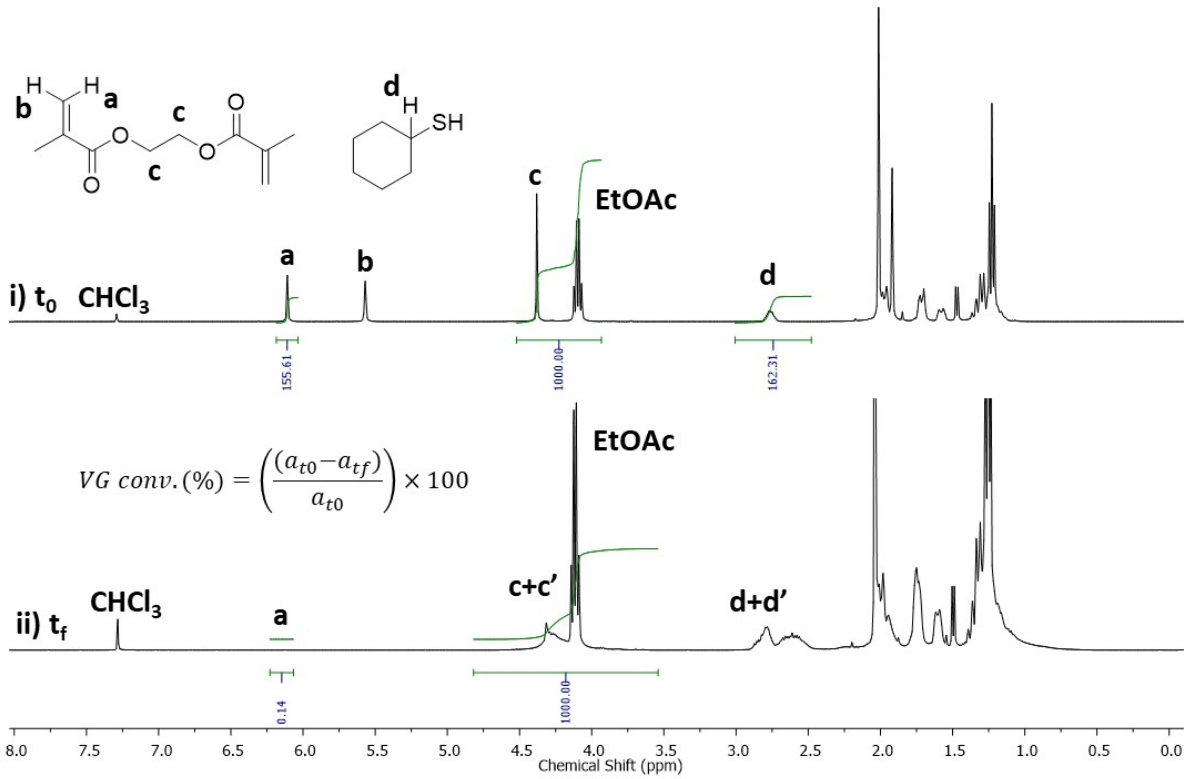


**Figure S5** Overlaid $^1$H NMR (400 MHz, $CDCl_3$) spectra obtained from the TBRT of EGDMA with CHT i) prior to initiation ($t_0$) and ii) 24 hours after later ($t_f$). The equation provided was used to determine vinyl conversion.

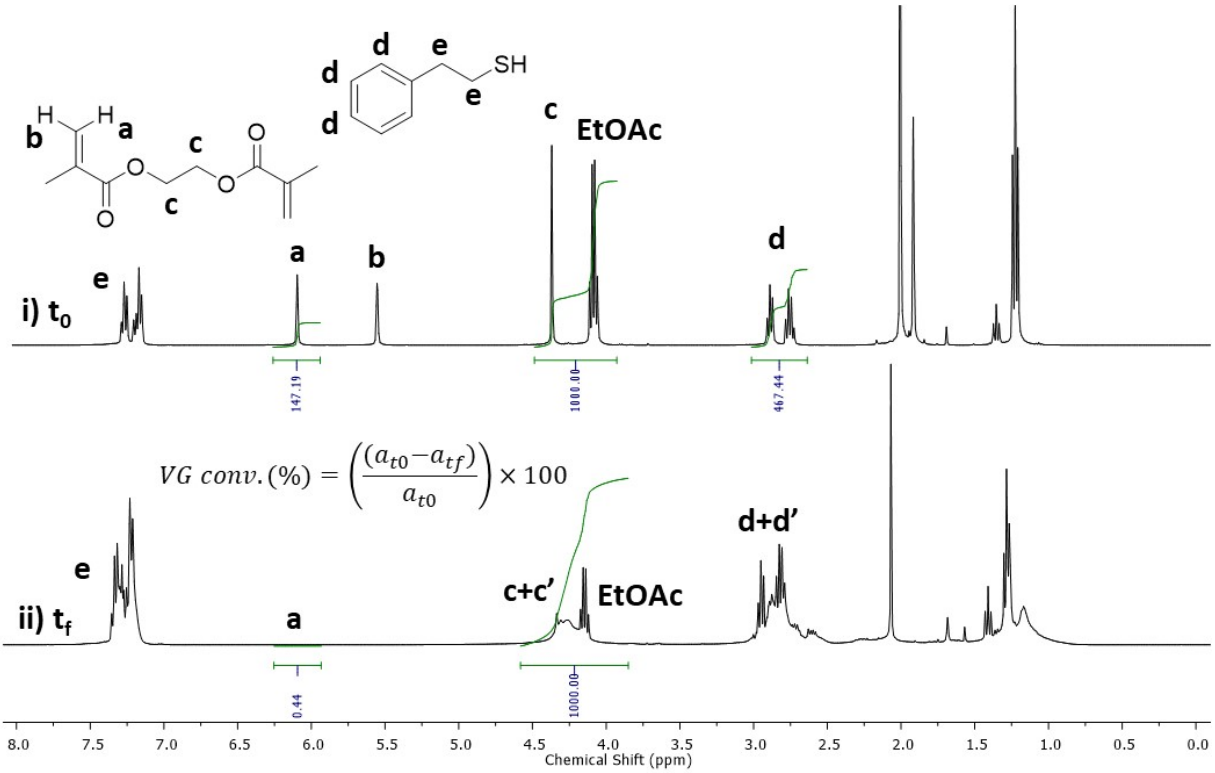


**Figure S6** Overlaid $^1$H NMR (400 MHz, $CDCl_3$) spectra obtained from the TBRT of EGDMA with PhEM i) prior to initiation ($t_0$) and ii) 24 hours after later ($t_f$). The equation provided was used to determine vinyl conversion.

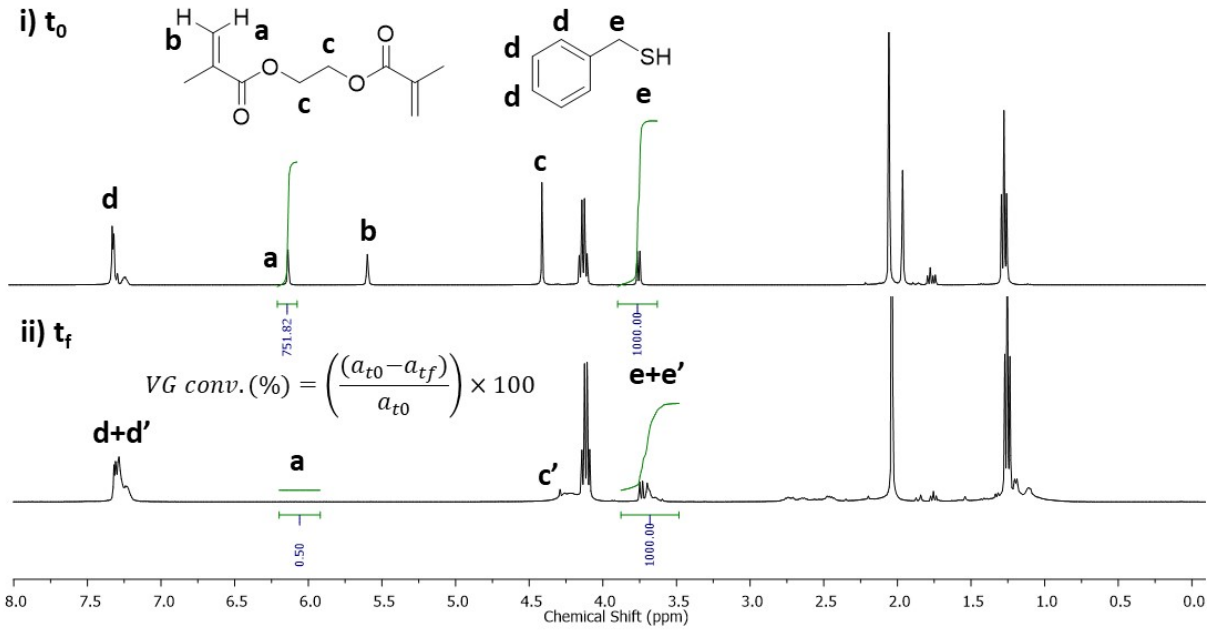


**Figure S7** Overlaid $^1$H NMR (400 MHz, $CDCl_3$) spectra obtained from TBRT of EGDMA with BzM i) prior to initiation ($t_0$) and ii) 24 hours after later ($t_f$). The equation provided was used to determine vinyl conversion.

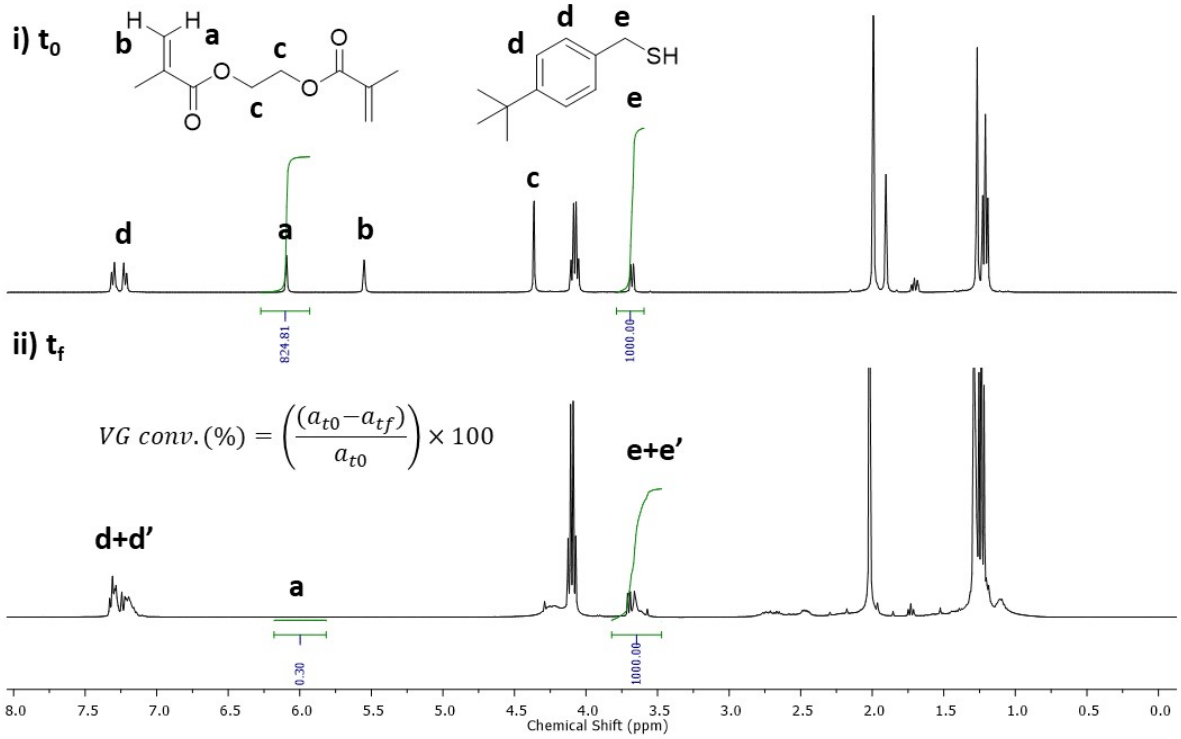


**Figure S8** Overlaid $^{1}$H NMR (400 MHz, $CDCl_3$) spectra obtained from TBRT of EGDMA with *t*BBM i) prior to initiation ($t_0$) and ii) 24 hours after later ($t_f$). The equation provided was used to determine vinyl conversion.

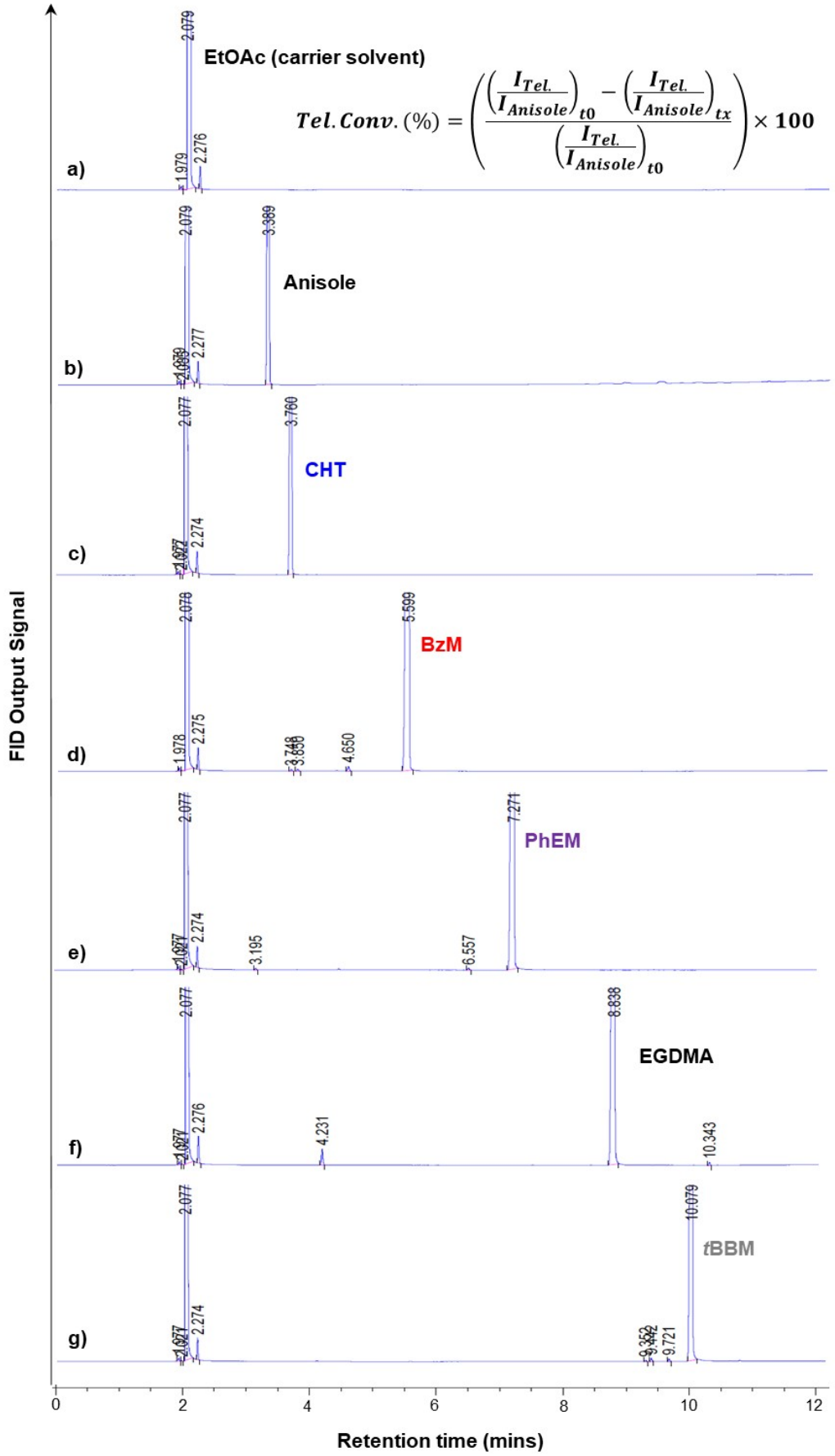


**Figure S9** Overlaid GC chromatograms obtained for a) EtOAc, b) anisole, c) CHT, d) BzM, e) PhEM, f) EGDMA and f) *t*BBM. The equation provided was used to determine both telogen and EGDMA conversion.

**Table S2** Kinetic monitoring of the TBRT of EGDMA and BzM ($[EGDMA]_0/[Tel]_0 = 0.45$).

| | | $^1$H NMR ($CDCl_3$)[a] | | | GC[b] | | |
|---|---|---|---|---|---|---|---|
| **Telogen** | **Time (mins)** | **Vinyl conv. (%)** | **$ln[M]_0/[M]$** | **LOG(1-α)** | **EGDMA Conv. (%)** | **Telogen Conv. (%)** | **$Log([Tel]/[Tel]_0)$** |
| | 0 | 0 | 0.000 | 0.000 | 0 | 0 | 0.000 |
| | 3 | 0 | 0.002 | 0.001 | 1 | 0 | 0.000 |
| | 6 | 6 | 0.057 | 0.025 | 11 | 2 | 0.007 |
| | 9 | 12 | 0.132 | 0.057 | 22 | 4 | 0.019 |
| | 12 | 18 | 0.201 | 0.087 | 32 | 6 | 0.026 |
| | 15 | 25 | 0.282 | 0.122 | 41 | 8 | 0.035 |
| | 20 | 34 | 0.417 | 0.181 | 53 | 11 | 0.050 |
| | 25 | 43 | 0.559 | 0.243 | 64 | 15 | 0.070 |
| BzM | 30 | 50 | 0.685 | 0.297 | 72 | 17 | 0.083 |
| | 40 | 63 | 0.991 | 0.431 | 85 | 29 | 0.146 |
| | 50 | 75 | 1.369 | 0.594 | 93 | 29 | 0.150 |
| | 60 | 85 | 1.895 | 0.823 | 97 | 34 | 0.181 |
| | 75 | 92 | 2.571 | 1.117 | 99 | 40 | 0.220 |
| | 90 | 97 | 3.405 | 1.479 | >99 | 43 | 0.247 |
| | 105 | 99 | 4.292 | 1.864 | >99 | 44 | 0.255 |
| | 120 | 99 | 4.949 | 2.149 | >99 | 45 | 0.258 |
| | 180 | >99 | 6.908 | 3.000 | >99 | 46 | 0.272 |

[a] Determined by 1H NMR analysis of the reaction mixture at the stated time intervals. [a] Determined by GC analysis of the reaction mixture at the stated time intervals.

**Table S3** Kinetic monitoring of the TBRT of EGDMA and *t*BBM ($[EGDMA]_0/[Tel]_0 = 0.45$).

| | | $^1$H NMR ($CDCl_3$)[a] | | | GC[b] | | |
|---|---|---|---|---|---|---|---|
| **Telogen** | **Time (mins)** | **Vinyl conv. (%)** | **$ln[M]_0/[M]$** | **Log(1-α)** | **EGDMA Conv. (%)** | **Telogen Conv. (%)** | **$Log([Tel]/[Tel]_0)$** |
| | 0 | 0 | 0.000 | 0.000 | 0 | 0 | 0.000 |
| | 3 | 0 | 0.000 | 0.000 | 1 | 0 | 0.000 |
| | 6 | 0 | 0.001 | 0.000 | 7 | 0 | 0.000 |
| | 9 | 0 | 0.003 | 0.001 | 13 | 0 | 0.000 |
| | 12 | 3 | 0.025 | 0.011 | 19 | 1 | 0.003 |
| | 15 | 27 | 0.315 | 0.137 | 26 | 2 | 0.007 |
| | 20 | 17 | 0.186 | 0.081 | 37 | 5 | 0.022 |
| | 25 | 22 | 0.249 | 0.108 | 48 | 7 | 0.034 |
| *t*BBM | 30 | 25 | 0.293 | 0.127 | 57 | 10 | 0.048 |
| | 40 | 44 | 0.575 | 0.250 | 71 | 16 | 0.075 |
| | 50 | 53 | 0.756 | 0.328 | 81 | 20 | 0.099 |
| | 60 | 60 | 0.905 | 0.393 | 89 | 26 | 0.129 |
| | 75 | 78 | 1.522 | 0.661 | 95 | 32 | 0.168 |
| | 90 | 85 | 1.914 | 0.831 | 98 | 38 | 0.207 |
| | 105 | 93 | 2.643 | 1.148 | >99 | 42 | 0.235 |
| | 120 | 95 | 3.062 | 1.330 | >99 | 42 | 0.236 |
| | 180 | >99 | 6.908 | 3.000 | >99 | 47 | 0.272 |

[a] Determined by 1H NMR analysis of the reaction mixture at the stated time intervals. [a] Determined by GC analysis of the reaction mixture at the stated time intervals.

**Table S4** Kinetic monitoring of the TBRT of EGDMA and CHT ($[EGDMA]_0/[Tel]_0 = 0.45$).

| Telogen | Time (mins) | $^1$H NMR ($CDCl_3$)[a] | | | GC[b] | | |
|---|---|---|---|---|---|---|---|
| | | Vinyl conv. (%) | $\ln[M]_0/[M]$ | LOG(1-α) | EGDMA Conv. (%) | Telogen Conv. (%) | $\text{Log}([Tel]/[Tel]_0)$ |
| CHT | 0 | 0 | 0.000 | 0.000 | 0 | 0 | 0.000 |
| | 3 | 0 | 0.000 | 0.000 | 1 | 0 | 0.000 |
| | 6 | 0 | 0.000 | 0.000 | 6 | 0 | 0.000 |
| | 9 | 0 | 0.000 | 0.000 | 11 | 0 | 0.001 |
| | 12 | 3 | 0.034 | 0.015 | 19 | 2 | 0.007 |
| | 15 | 10 | 0.100 | 0.043 | 25 | 3 | 0.012 |
| | 20 | 20 | 0.226 | 0.098 | 39 | 5 | 0.022 |
| | 25 | 29 | 0.342 | 0.148 | 50 | 7 | 0.033 |
| | 30 | 35 | 0.428 | 0.186 | 60 | 10 | 0.044 |
| | 40 | 53 | 0.745 | 0.324 | 77 | 15 | 0.068 |
| | 50 | 67 | 1.102 | 0.479 | 88 | 20 | 0.095 |
| | 60 | 78 | 1.505 | 0.654 | 95 | 24 | 0.119 |
| | 120 | >99 | 5.642 | 2.450 | >99 | 36 | 0.193 |

[a] Determined by 1H NMR analysis of the reaction mixture at the stated time intervals. [a] Determined by GC analysis of the reaction mixture at the stated time intervals.

**Table S5** Kinetic monitoring of the TBRT of EGDMA and PhEM ($[EGDMA]_0/[Tel]_0 = 0.45$).

| Telogen | Time (mins) | $^1$H NMR ($CDCl_3$)[a] | | | GC[b] | | |
|---|---|---|---|---|---|---|---|
| | | Vinyl conv. (%) | $\ln[M]_0/[M]$ | LOG(1-α) | EGDMA Conv. (%) | Telogen Conv. (%) | $\text{Log}([Tel]/[Tel]_0)$ |
| PhEM | 0 | 0 | 0.000 | 0.000 | 0 | 0 | 0.000 |
| | 3 | 0 | 0.000 | 0.000 | 4 | 0 | 0.000 |
| | 6 | 2 | 0.020 | 0.009 | 11 | 0 | 0.000 |
| | 9 | 3 | 0.025 | 0.011 | 20 | 1 | 0.005 |
| | 12 | 6 | 0.058 | 0.025 | 27 | 2 | 0.011 |
| | 15 | 13 | 0.142 | 0.062 | 37 | 5 | 0.022 |
| | 20 | 23 | 0.267 | 0.116 | 50 | 7 | 0.034 |
| | 25 | 34 | 0.416 | 0.181 | 61 | 11 | 0.049 |
| | 30 | 41 | 0.533 | 0.232 | 71 | 13 | 0.061 |
| | 40 | 59 | 0.884 | 0.384 | 85 | 20 | 0.095 |
| | 50 | 72 | 1.257 | 0.546 | 93 | 25 | 0.125 |
| | 60 | 82 | 1.723 | 0.748 | 97 | 30 | 0.154 |
| | 75 | 93 | 2.630 | 1.142 | >99 | 36 | 0.190 |
| | 90 | 98 | 3.847 | 1.671 | >99 | 39 | 0.213 |
| | 105 | 99 | 4.914 | 2.134 | >99 | 40 | 0.220 |
| | 120 | >99 | 6.452 | 2.802 | >99 | 39 | 0.217 |
| | 180 | >99 | 6.908 | 3.000 | >99 | 39 | 0.217 |

[a] Determined by 1H NMR analysis of the reaction mixture at the stated time intervals. [a] Determined by GC analysis of the reaction mixture at the stated time intervals.

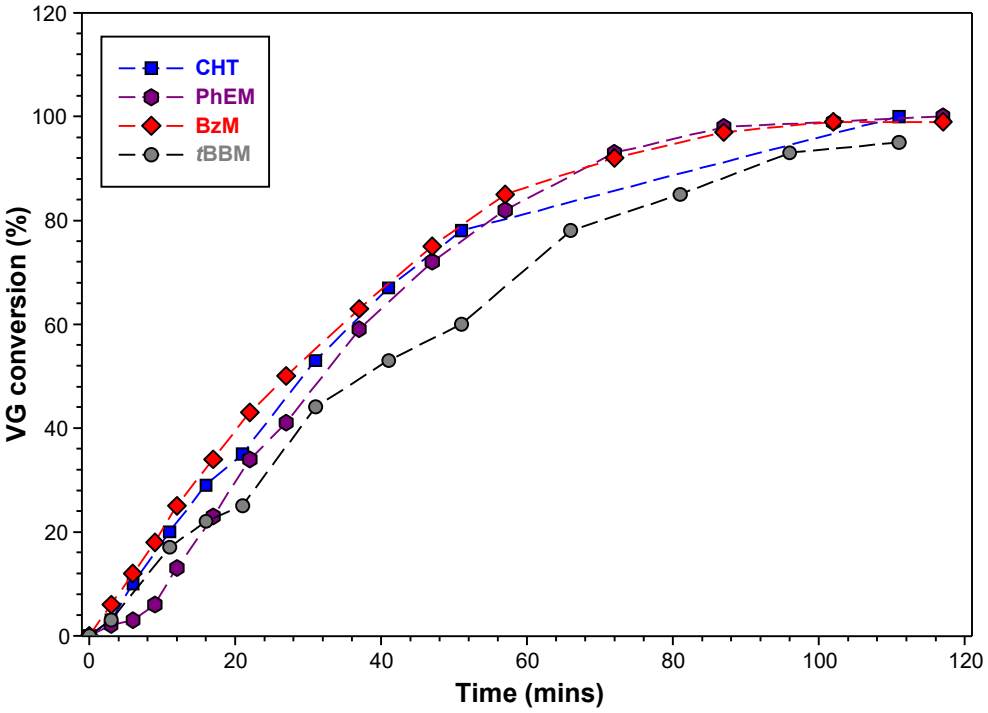


**Figure S10** Induction period-adjusted kinetic plots of vinyl consumption with time during TBRTs of EGDMA with a) CHT (blue squares), b) PhEM (purple hexagons), c) BzM (red diamonds) and d) *t*BBM (dark grey circles).

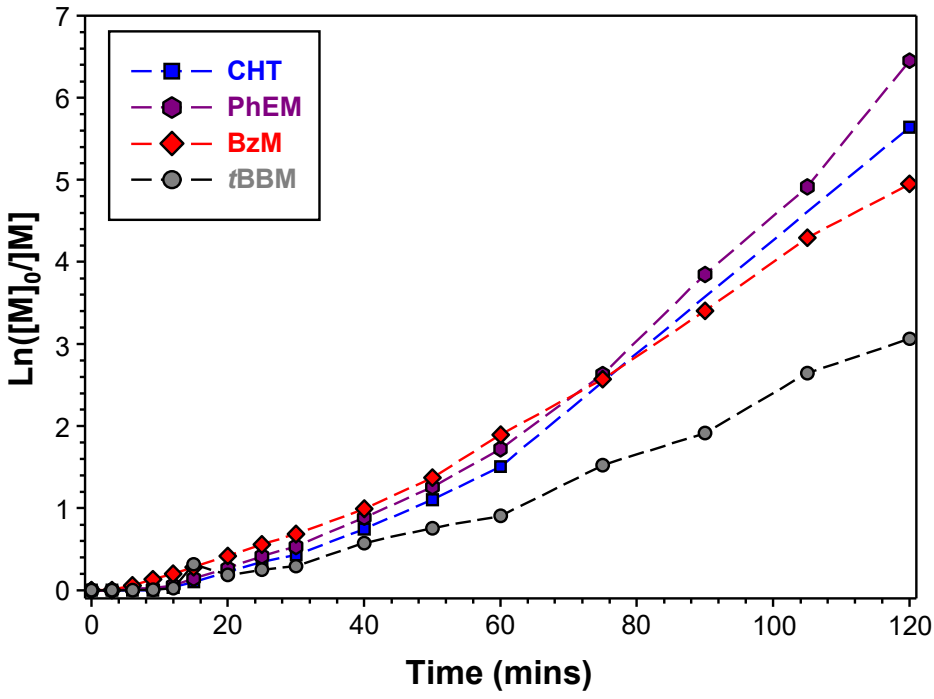


**Figure S11** Overlaid semi-logarithmic plots of vinyl conversion during TBRTs of EGDMA with a) CHT (blue squares), b) PhEM (purple hexagons), c) BzM (red diamonds) and d) *t*BBM (dark grey circles).

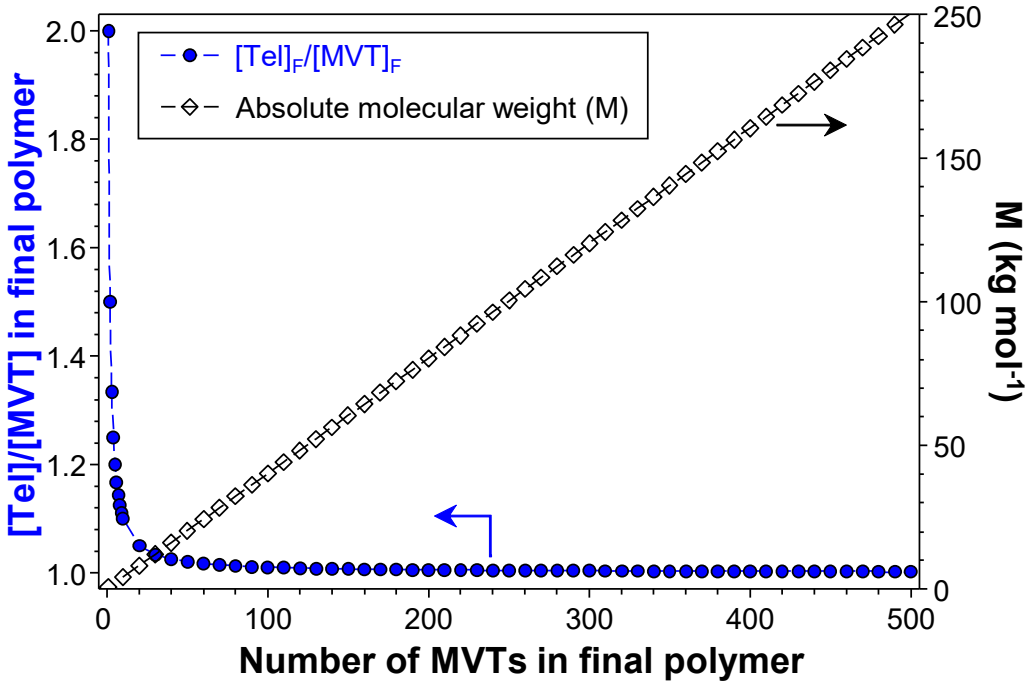


**Figure S12** Theoretical illustration of the expected variation in the molar ratio of telogen to multi-vinyl taxogen (MVT, i.e. EGDMA, blue circles) and absolute molecular weight (M, black hollow diamonds), as the number of MVTs in the branched polymer structure increase.

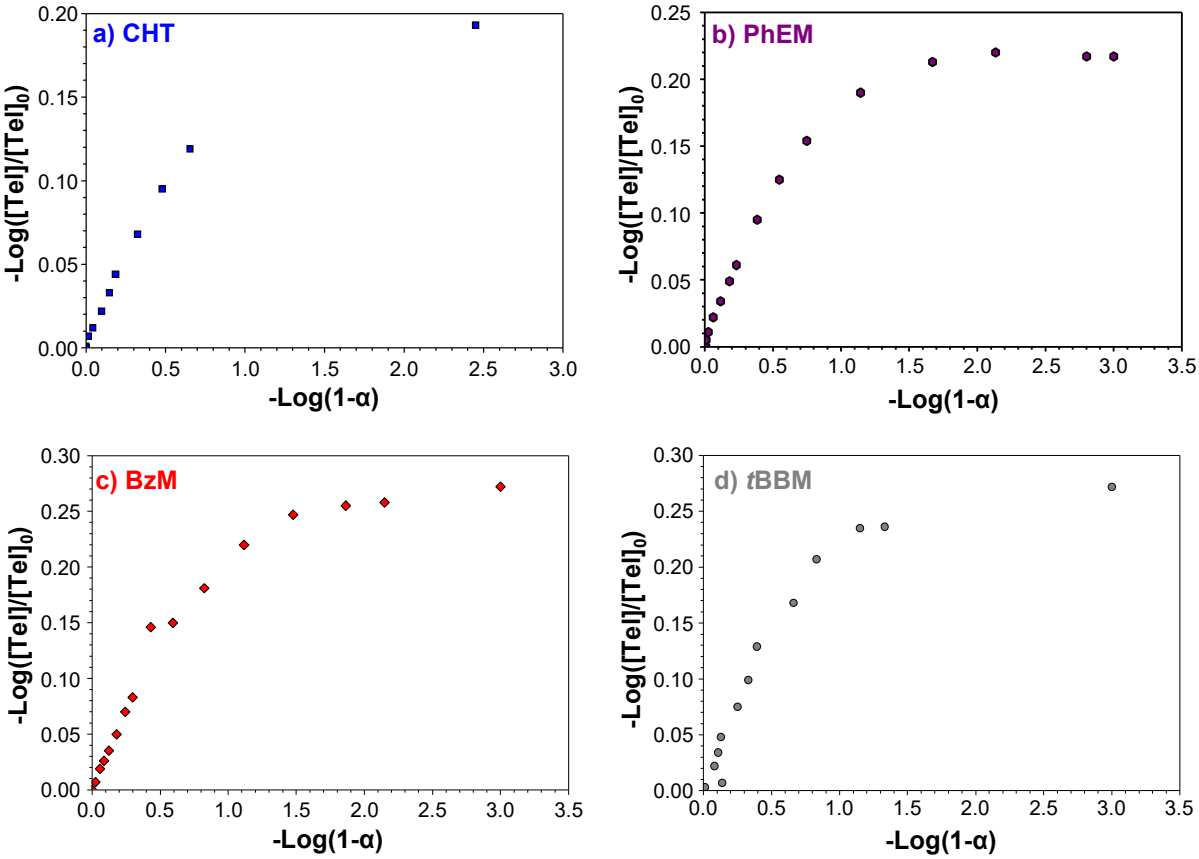


**Figure S13** Full plots of Log([Tel]/[Tel]$_0$) against Log(1-α) obtained from TBRTs of EGDMA with a) CHT, b) PhEM, c) BzM and d) *t*BBM.

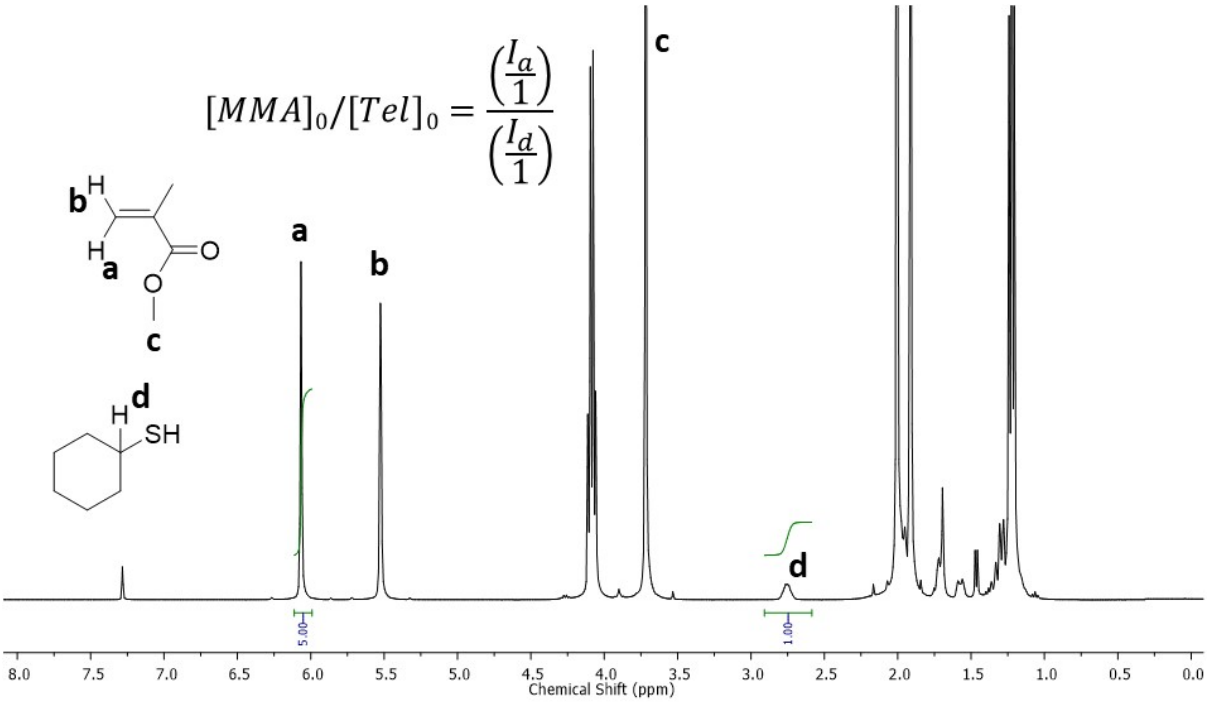


**Figure S14** $^1$H NMR (400 MHz, $CDCl_3$) spectrum obtained from the linear telomerisation of MMA with CHT prior to thermal initiation (t = 0). The equation provided was used to determine the initial ratio of MMA to CHT ($[MMA]_0/[Tel]_0$).

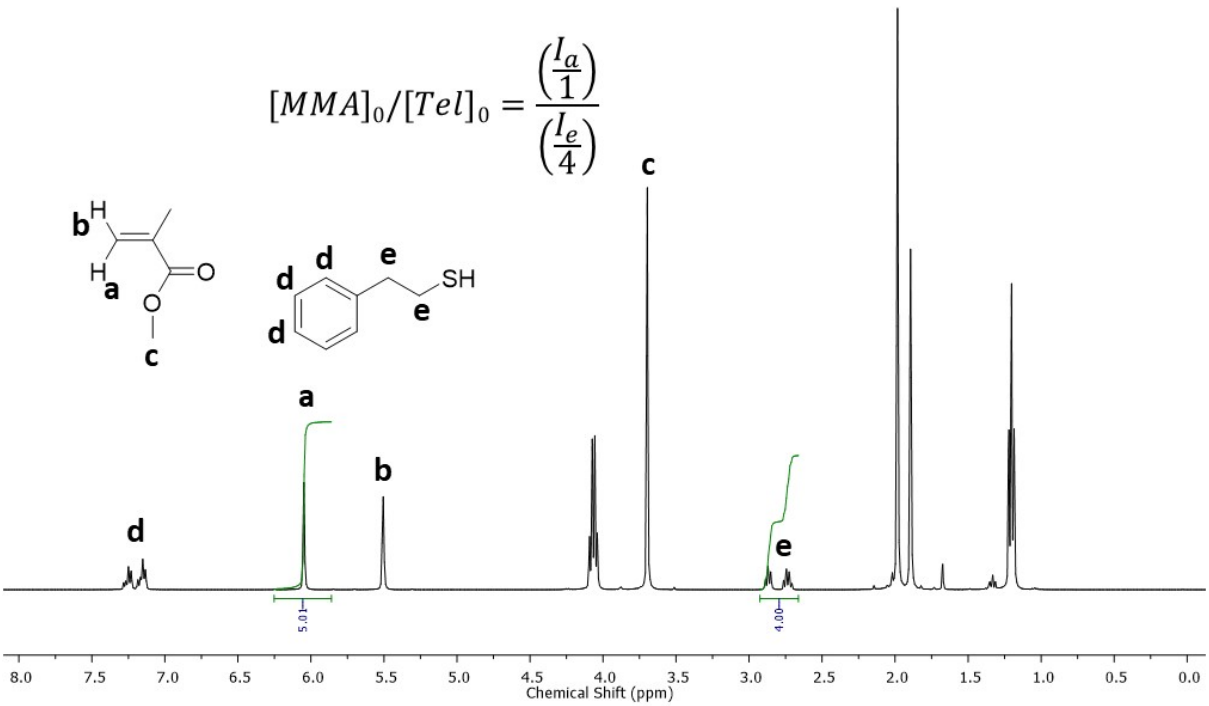


**Figure S15** $^1$H NMR (400 MHz, $CDCl_3$) spectrum obtained from the linear telomerisation of MMA with PhEM prior to thermal initiation (t = 0). The equation provided was used to determine the initial ratio of MMA to PhEM ($[MMA]_0/[Tel]_0$).

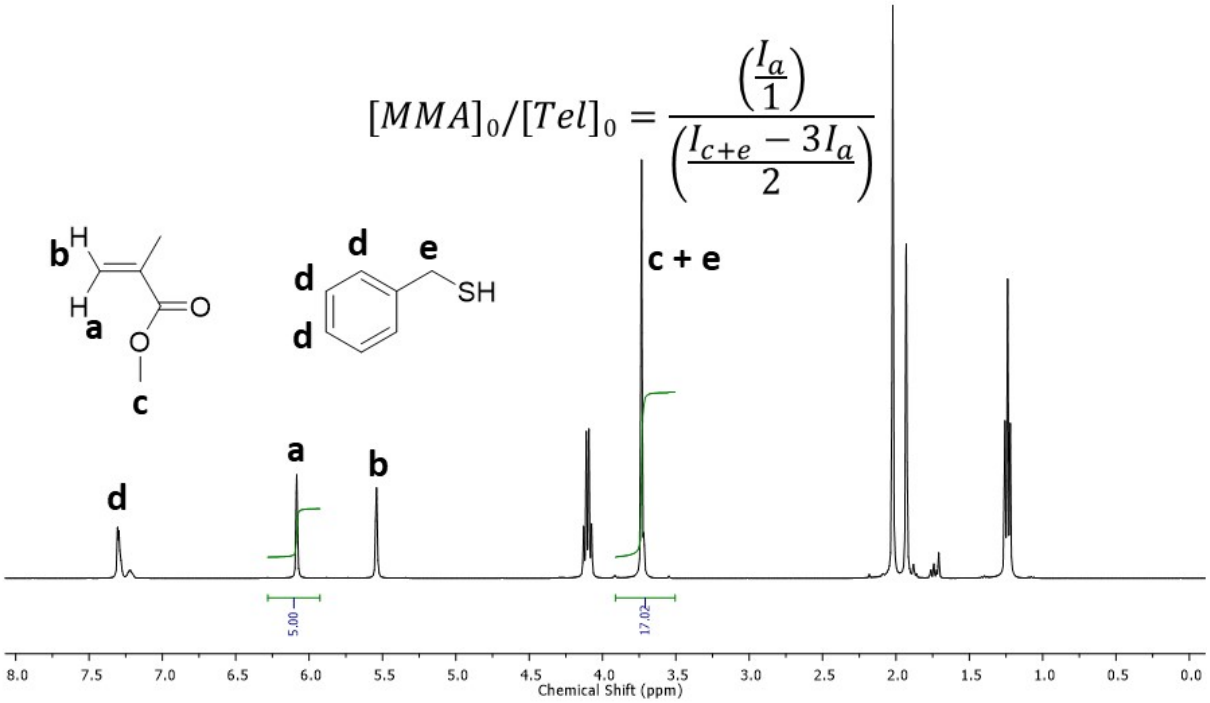


**Figure S16** $^1$H NMR (400 MHz, $CDCl_3$) spectrum obtained from the linear telomerisation of MMA with BzM prior to thermal initiation (t = 0). The equation provided was used to determine the initial ratio of MMA to BzM ($[MMA]_0/[Tel]_0$).

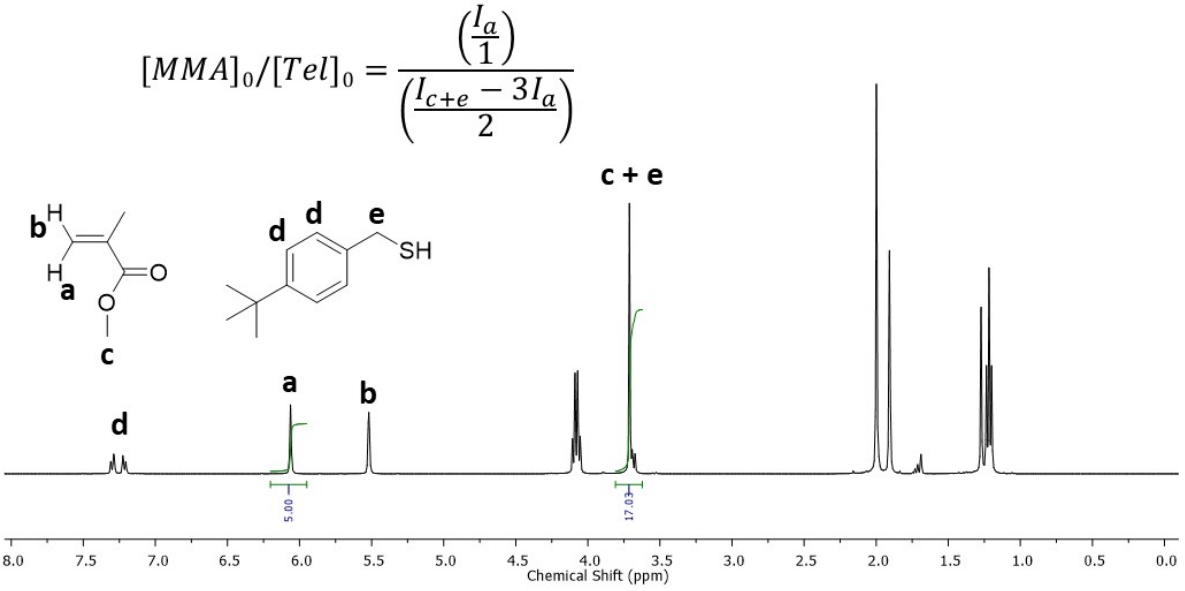


**Figure S17** $^1$H NMR (400 MHz, $CDCl_3$) spectrum obtained from the linear telomerisation of MMA with *t*BBM prior to thermal initiation (t = 0). The equation provided was used to determine the initial ratio of MMA to *t*BBM ($[MMA]_0/[Tel]_0$).

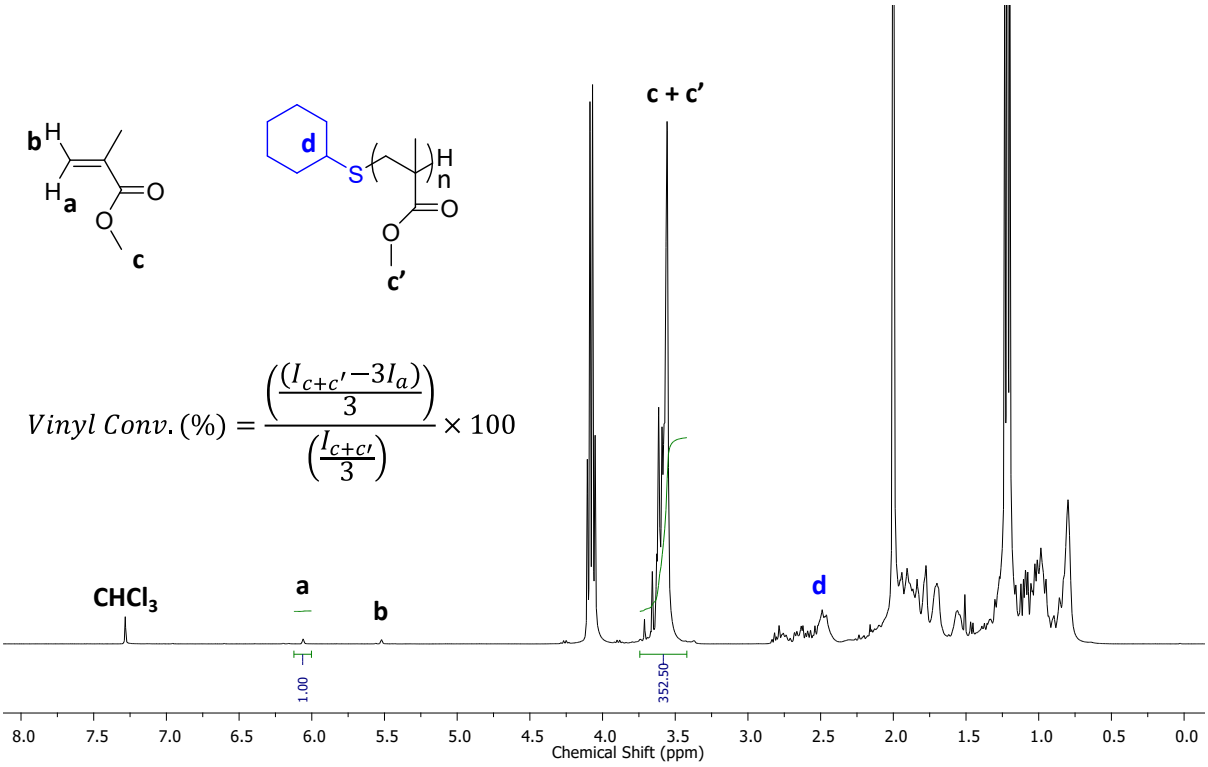


**Figure S18** $^1$H NMR (400 MHz, $CDCl_3$) spectrum obtained from the linear telomerisation of MMA with CHT after 24 hours ($t_f$). The equation provided was used to determine vinyl conversion.

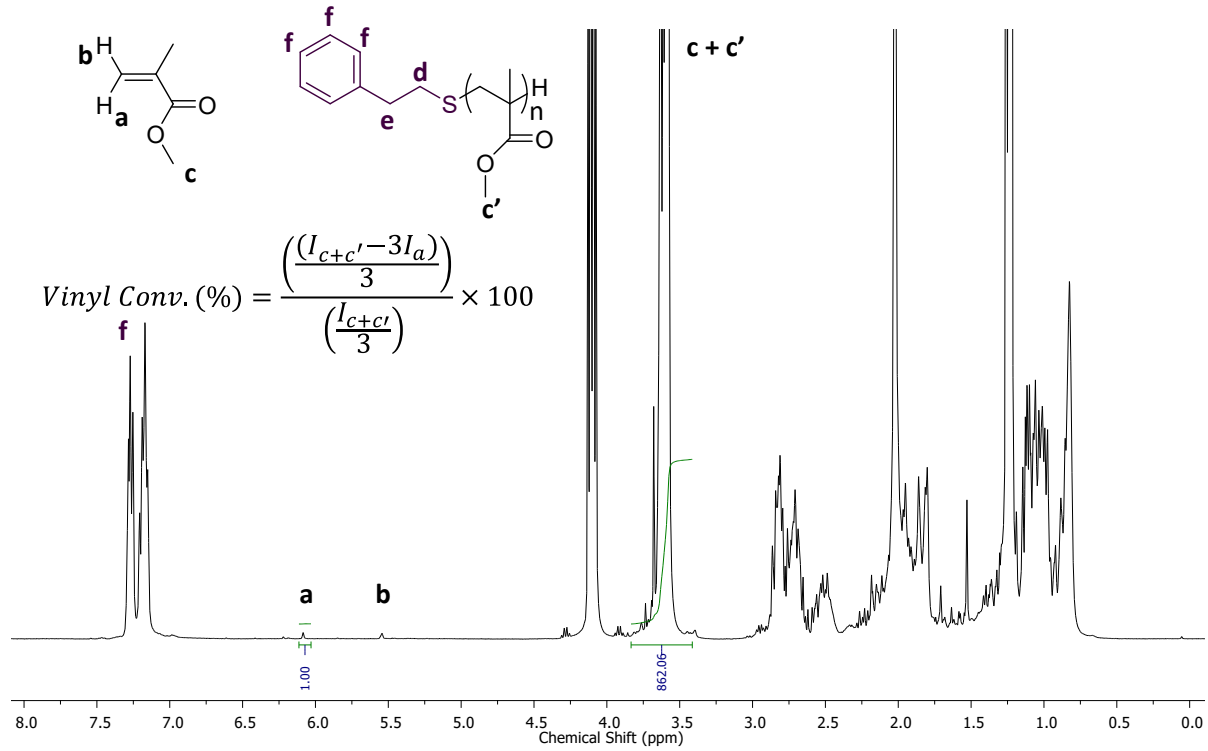


**Figure S19** $^1$H NMR (400 MHz, $CDCl_3$) spectrum obtained from the linear telomerisation of MMA with PhEM after 24 hours ($t_f$). The equation provided was used to determine vinyl conversion.

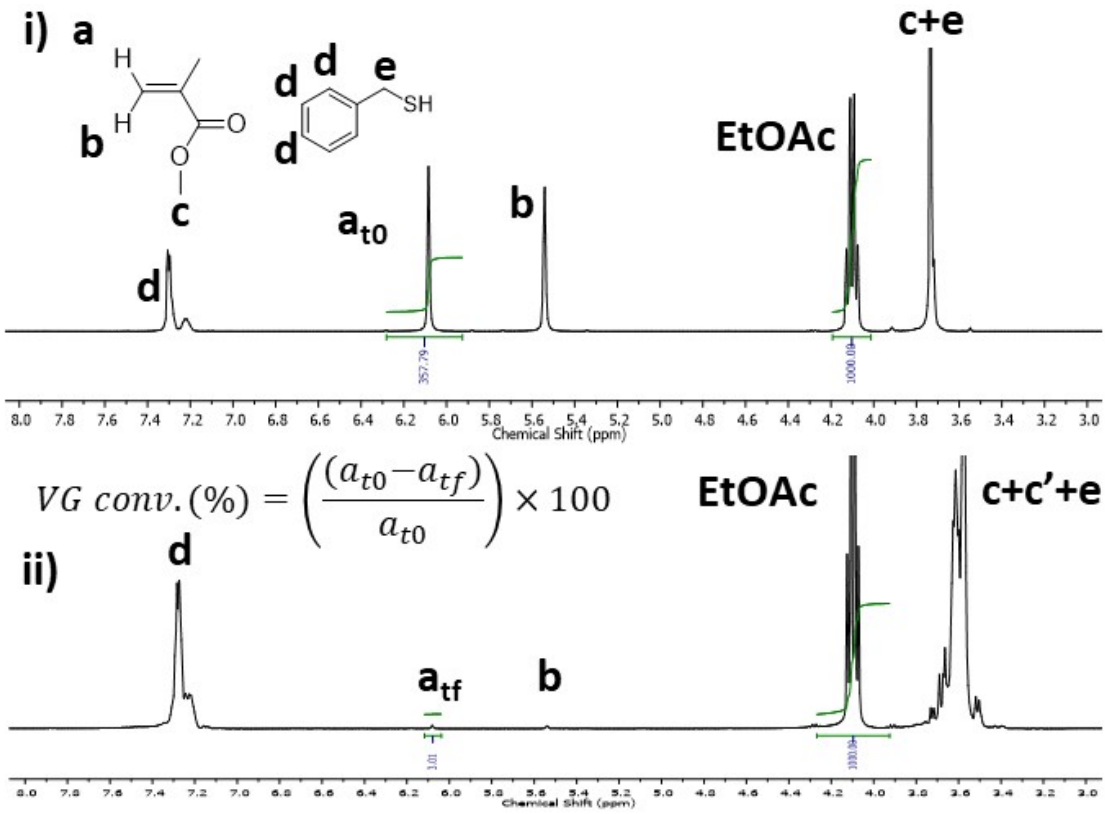


**Figure S20** Overlaid $^1$H NMR (400 MHz, $CDCl_3$) spectra obtained from the linear telomerisation of MMA with BzM i) prior to initiation and ii) 24 hours later ($t_f$). The equation provided was used to determine vinyl conversion.

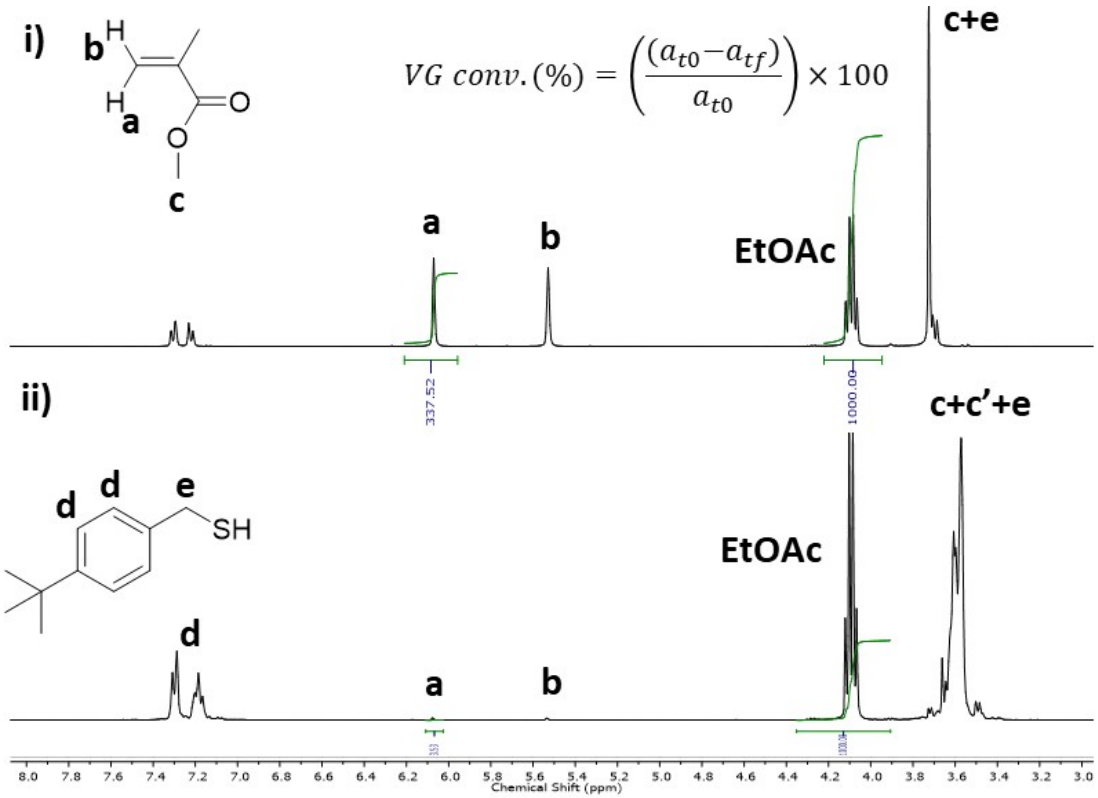


**Figure S21** Overlaid $^1$H NMR (400 MHz, $CDCl_3$) spectra obtained from the linear telomerisation of MMA with *t*BBM. i) prior to initiation and ii) 24 hours later ($t_f$). The equation provided was used to determine vinyl conversion.

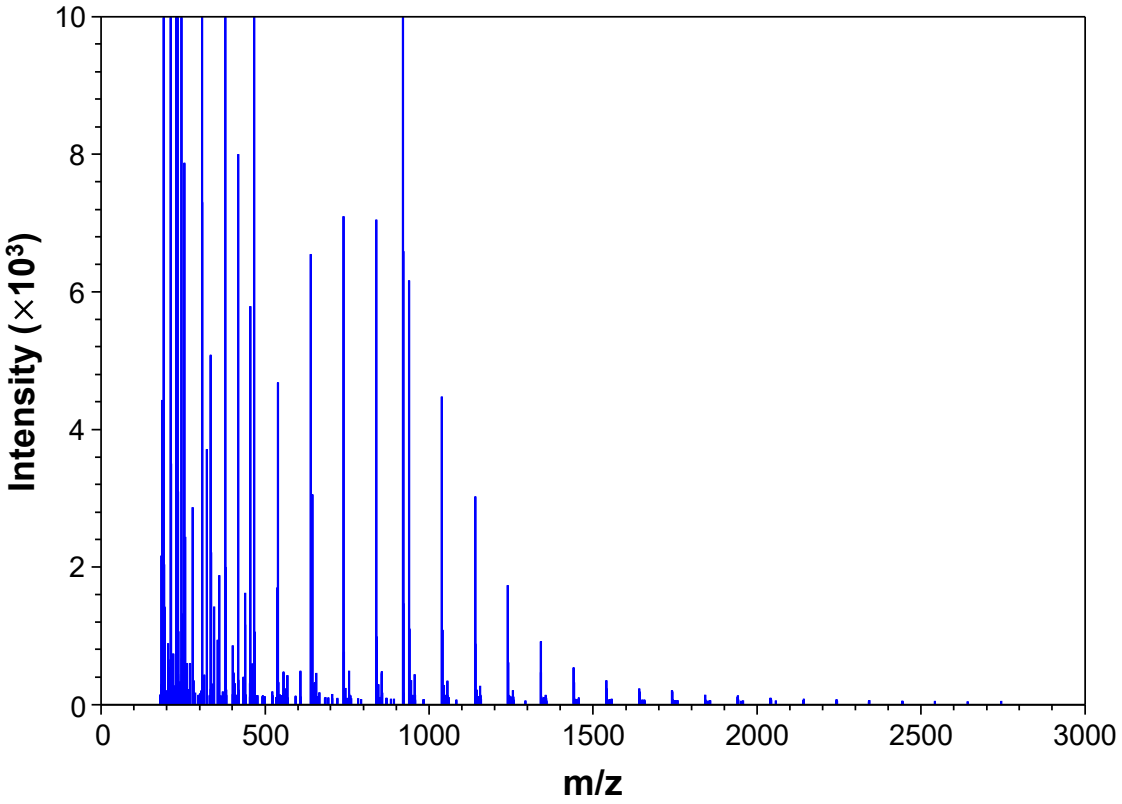


**Figure S22** Crude MALDI-TOF mass spectrum obtained for CHT-*p*(MMA).

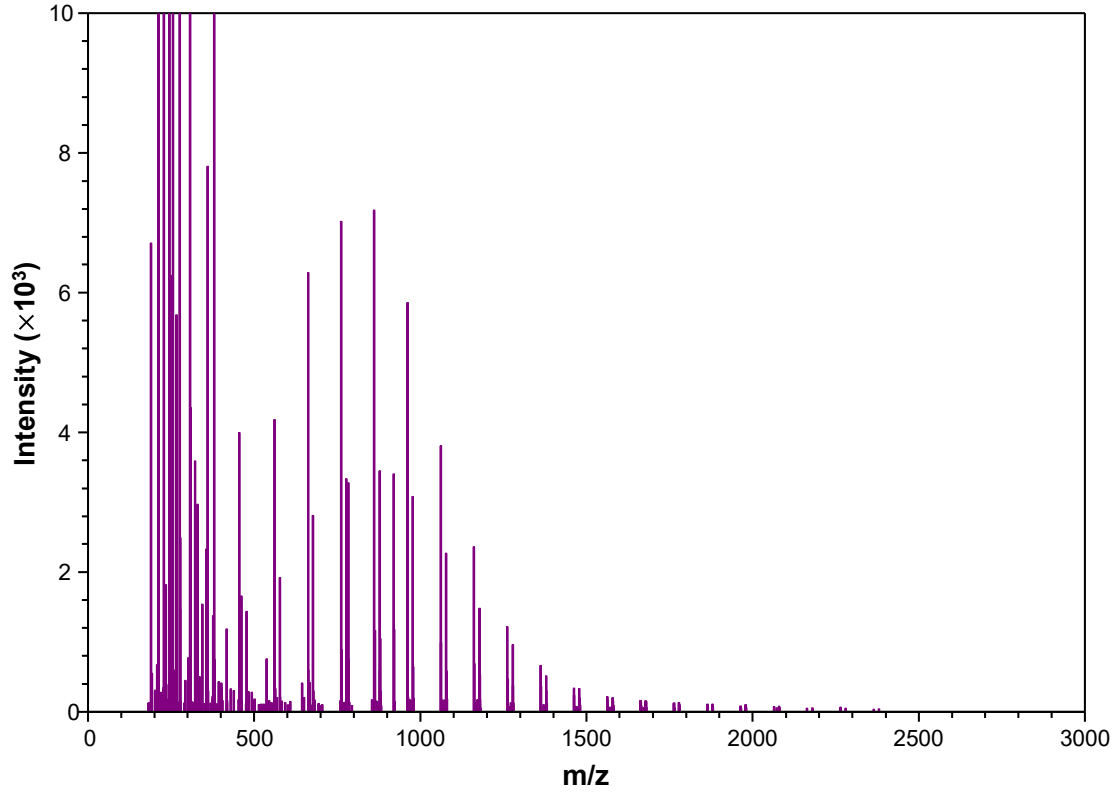


**Figure S23** Crude MALDI-TOF mass spectrum obtained for PhEM-*p*(MMA).

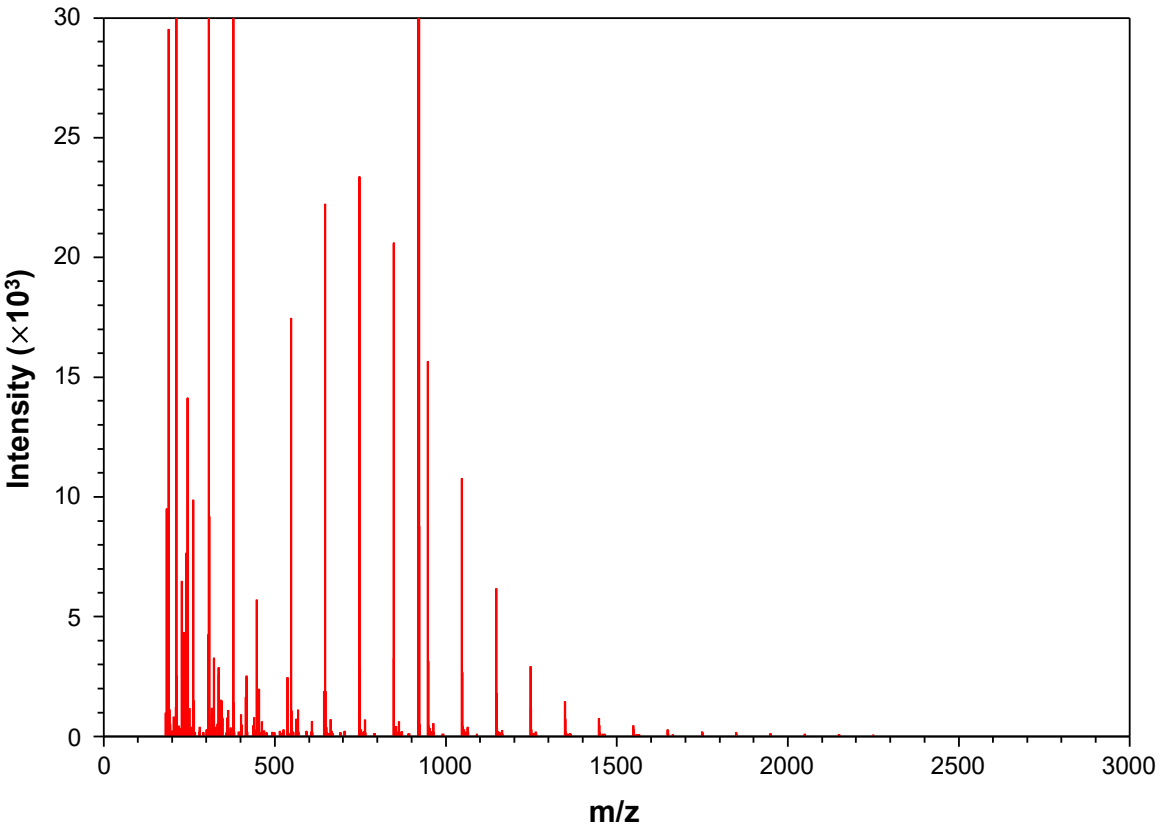


**Figure S24** Crude MALDI-TOF mass spectrum obtained for BzM-*p*(MMA).

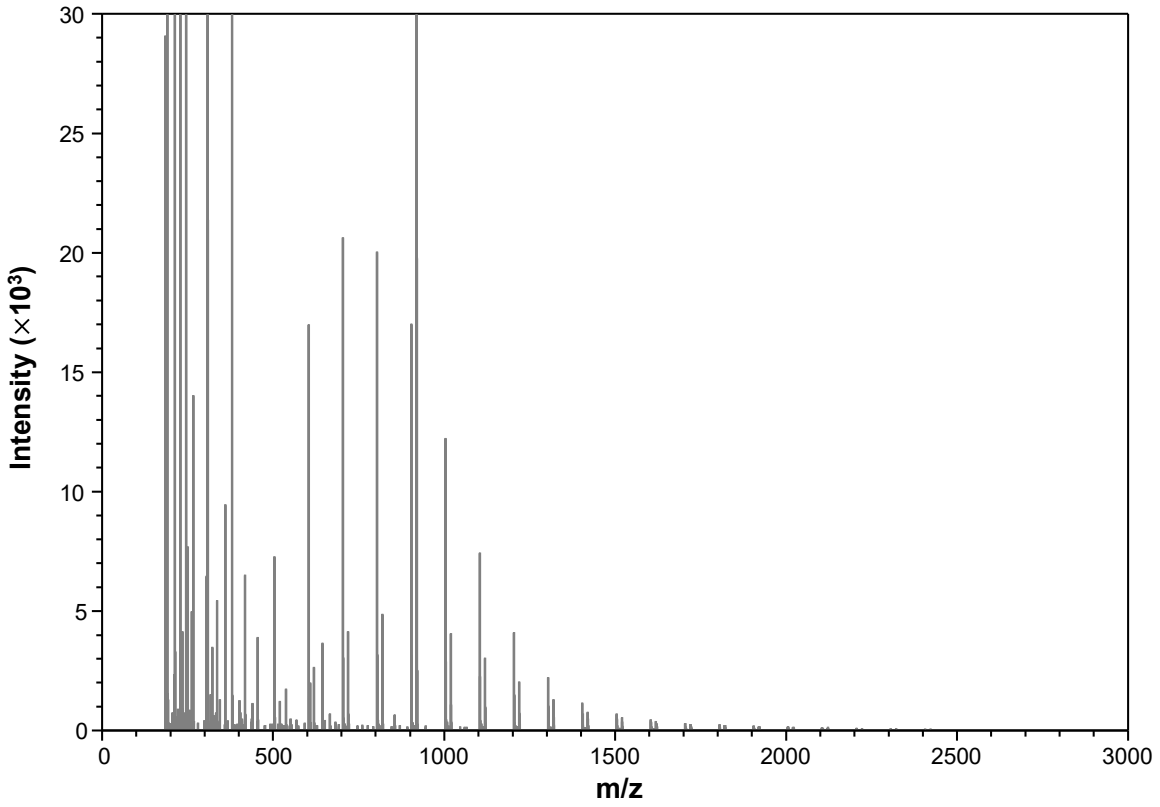


**Figure S25** Crude MALDI-TOF mass spectrum obtained for *t*BBM-*p*(MMA).

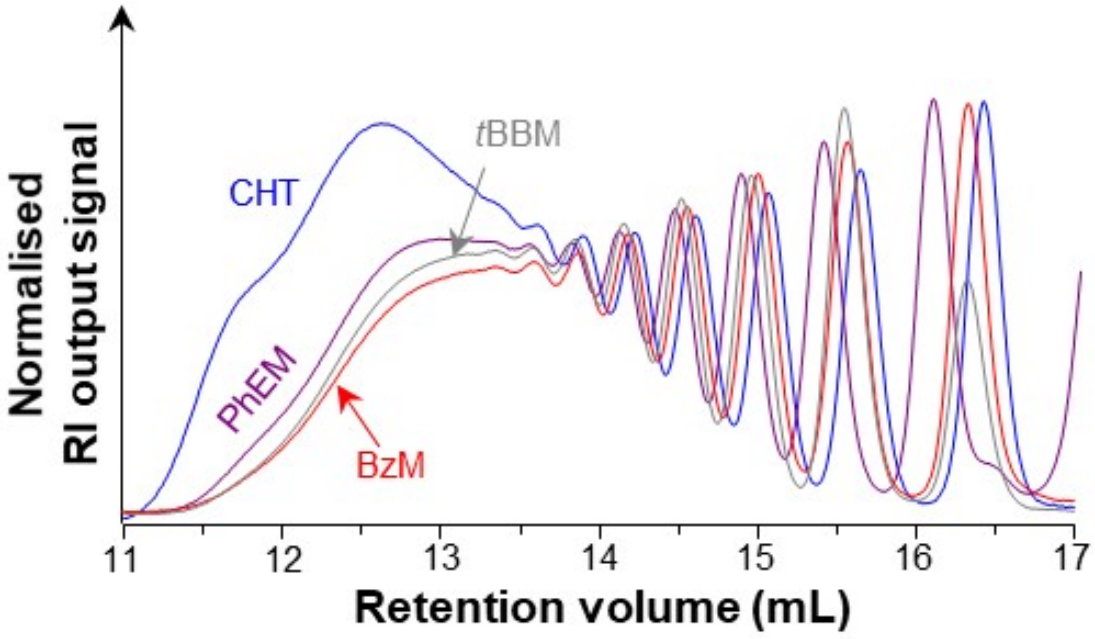


**Figure S26** Overlaid RI chromatograms of linear telomers obtained by SEC of linear telomers.

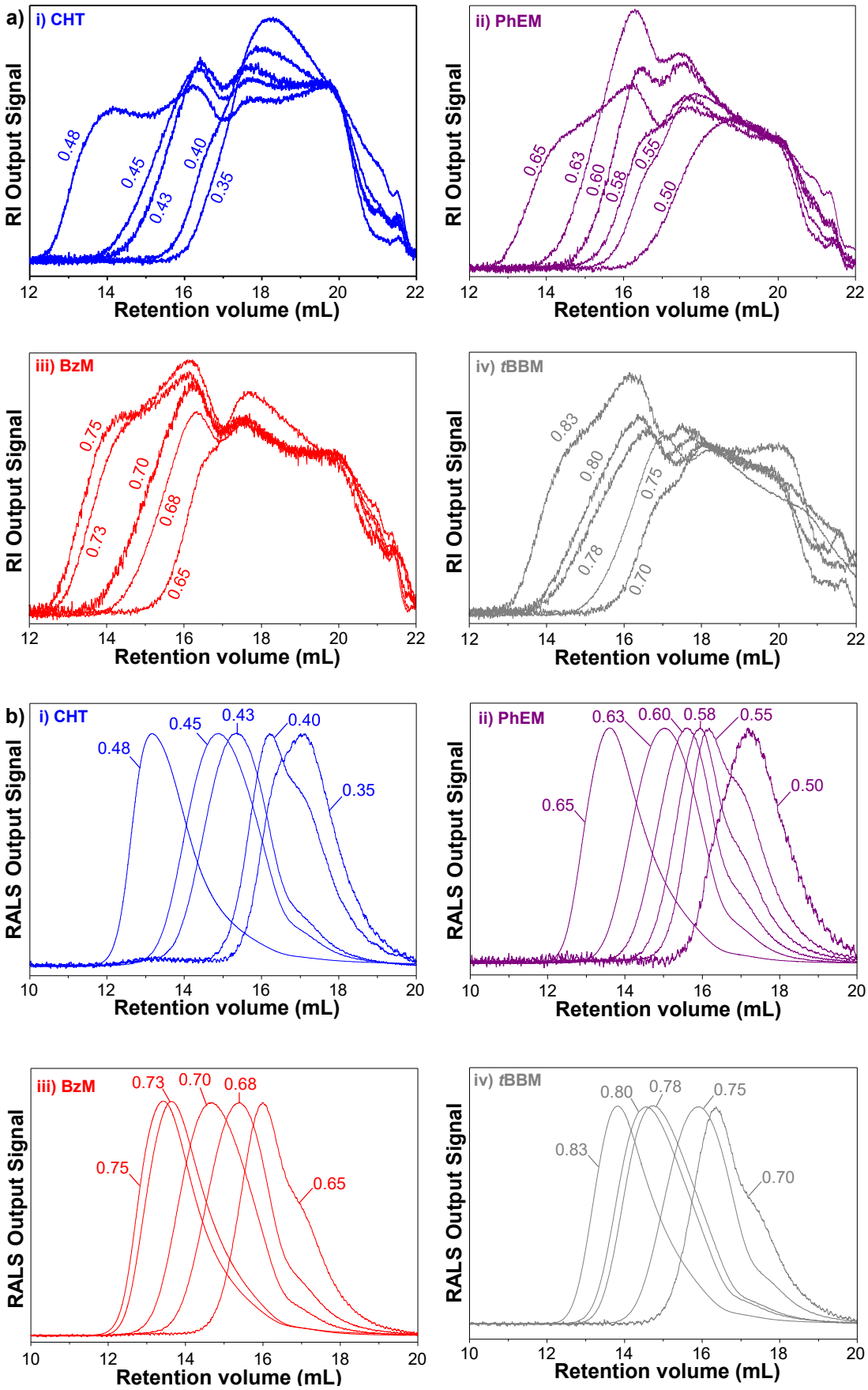


**Figure S27** Overlaid a) RI and b) RALS chromatograms obtained from TD-SEC analysis of i) *p*(CHT-EGDMA), ii) *p*(PhEM-EGDMA) and iii) *p*(BzM-EGDMA) and iv) *p*(*t*BBM-EGDMA) branched copolymers generated at varied $[EGDMA]_0/[Tel]_0$ ratios (stated on each chromatogram).

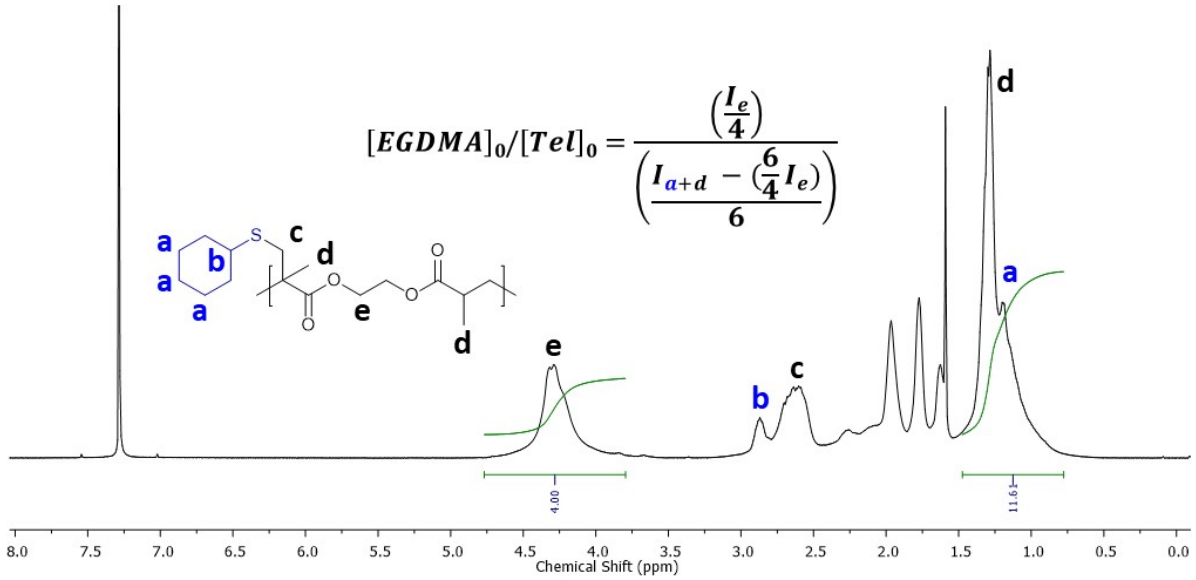


**Figure S28** Exemplary $^1$H NMR spectroscopic characterisation of *p*(CHT-EGDMA). The equation provided was used to determine the final molar ratio of EGDMA to CHT residues in the purified polymer ($[EGDMA]_F/[Tel]_F$).

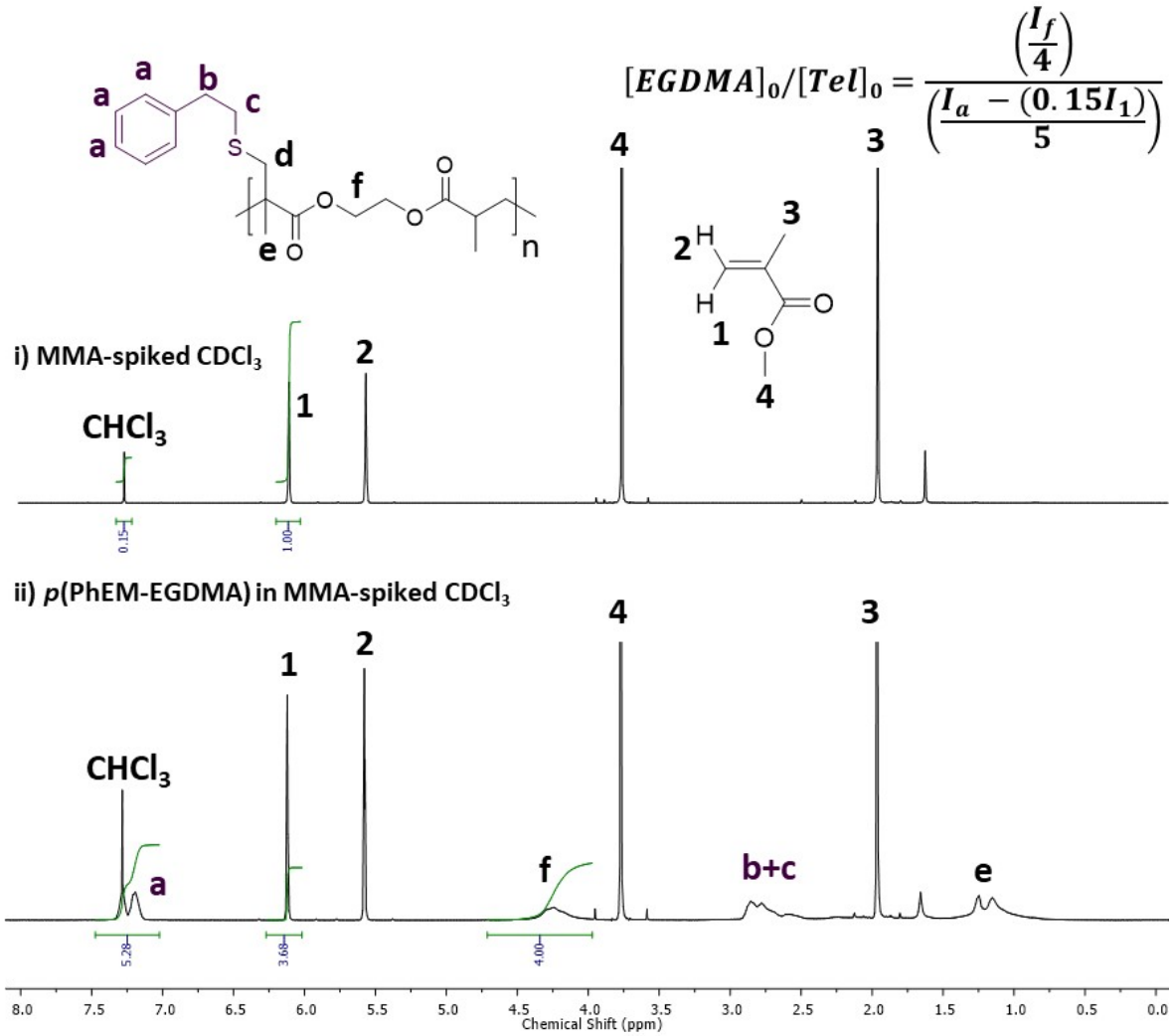


**Figure S29** Exemplary $^1$H NMR spectroscopic characterisation of *p*(PhEM-EGDMA). The equation provided was used to determine the final molar ratio of EGDMA to PhEM residues in the purified polymer ($[EGDMA]_F/[Tel]_F$).

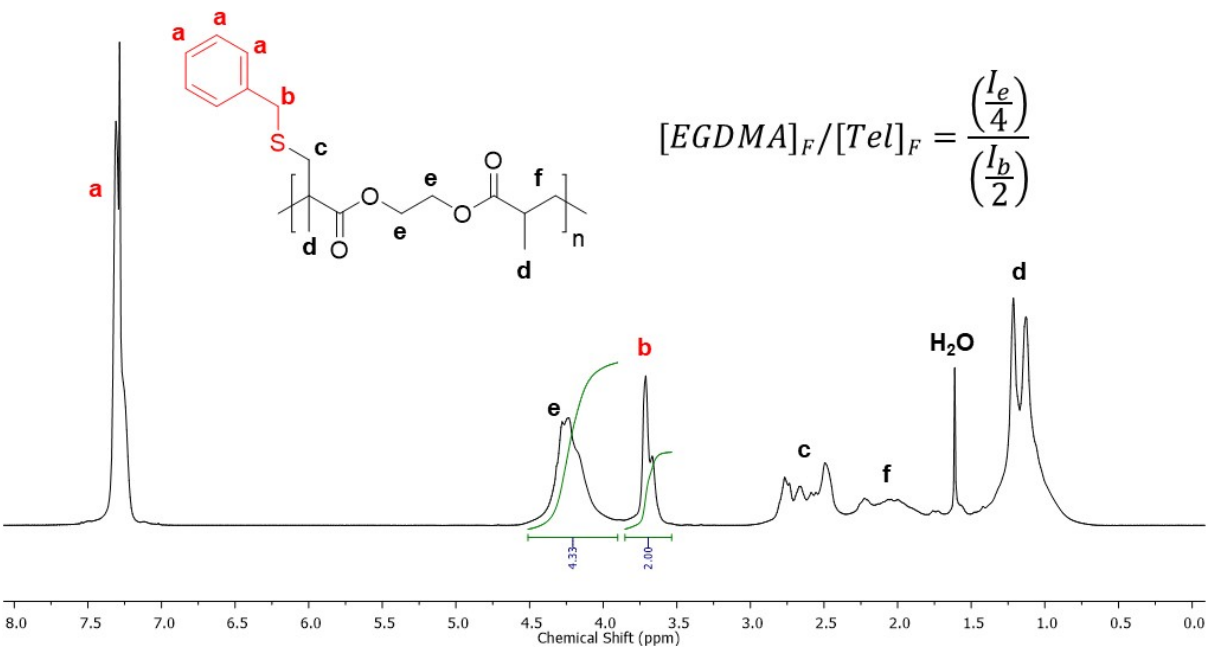


**Figure S30** Exemplary $^1$H NMR spectroscopic characterisation of *p*(BzM-EGDMA). The equation provided was used to determine the final molar ratio of EGDMA to BzM residues in the purified polymer ($[EGDMA]_F/[Tel]_F$).

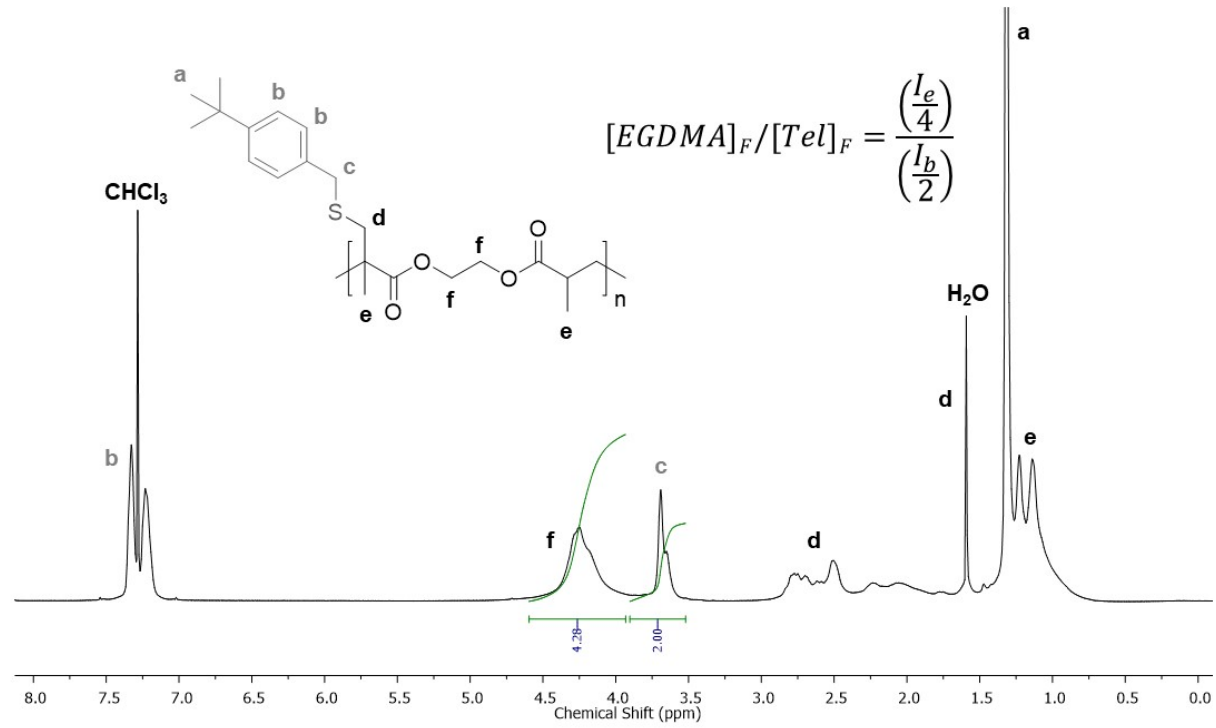


**Figure S31** Exemplary $^1$H NMR spectroscopic characterisation of *p*(*t*BBM-EGDMA). The equation provided was used to determine the final molar ratio of EGDMA to *t*BBM residues in the purified polymer ($[EGDMA]_F/[Tel]_F$).

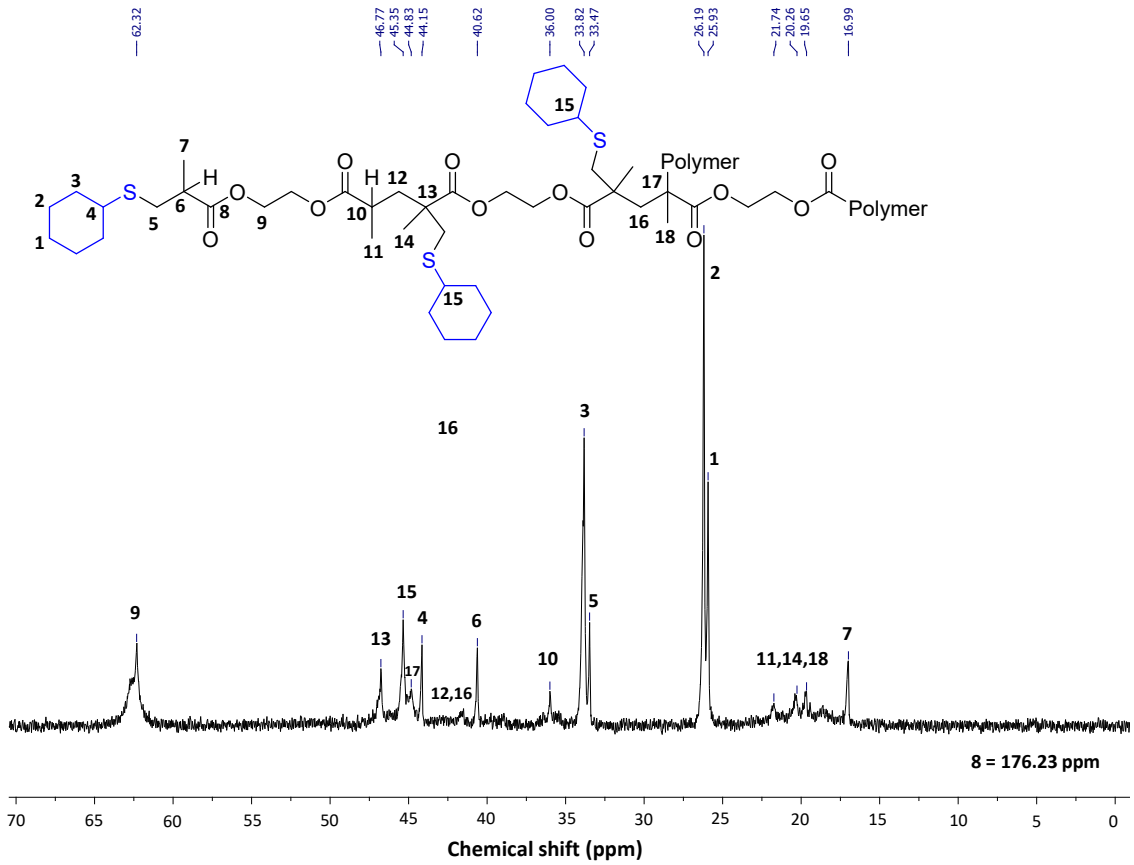


**Figure S32** $^{13}$C NMR spectroscopic characterisation of *p*(CHT-EGDMA).

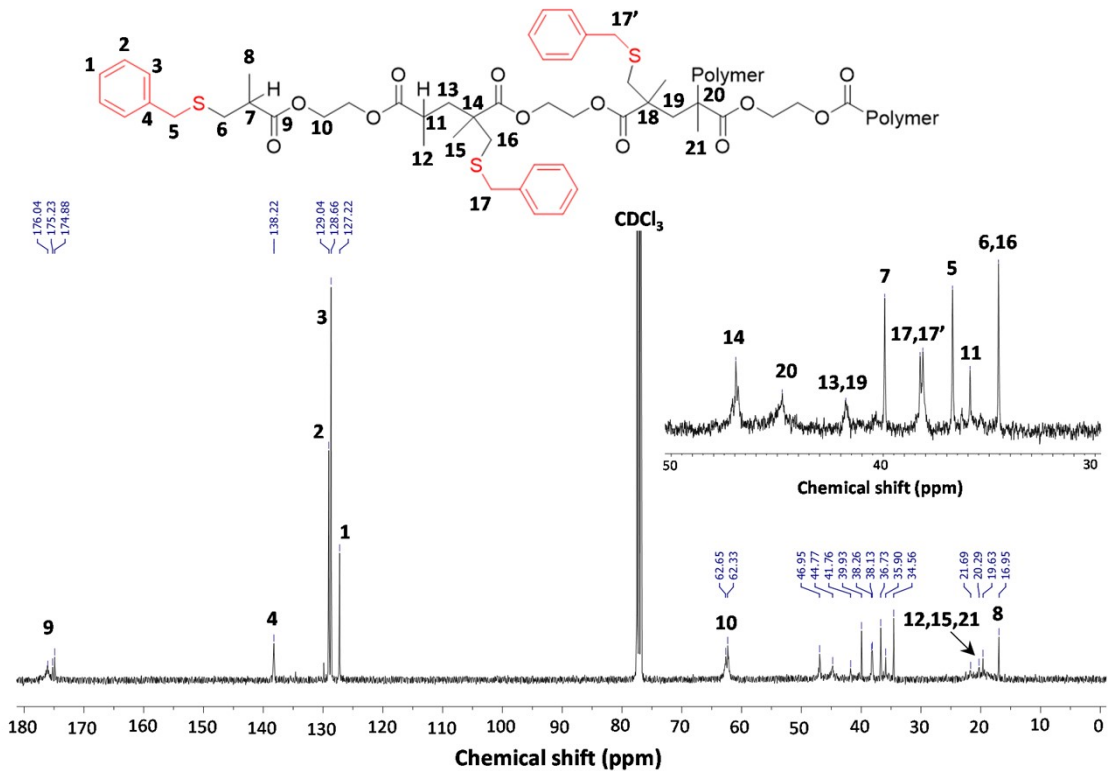


**Figure S33** $^{13}$C NMR spectroscopic characterisation of *p*(BzM-EGDMA).

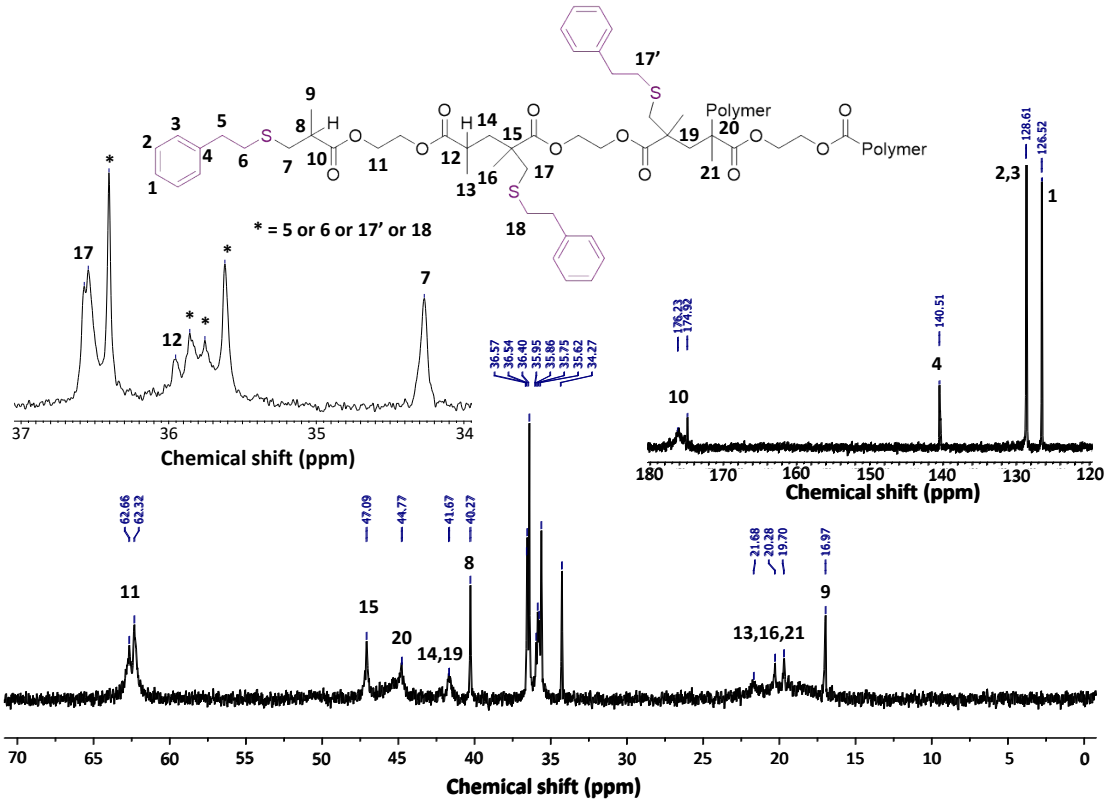


**Figure S34** $^{13}$C NMR spectroscopic characterisation of *p*(PhEM-EGDMA).

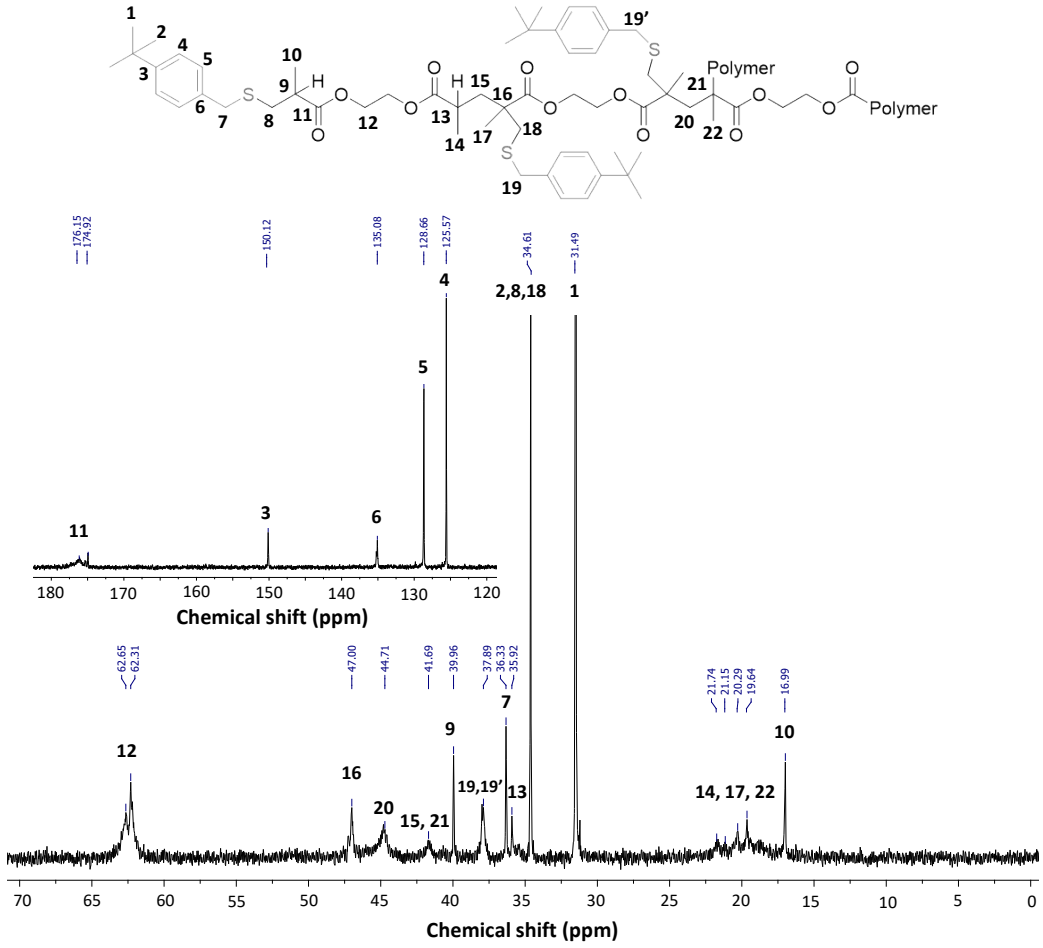


**Figure S35** $^{13}$C NMR spectroscopic characterisation of *p*(*t*BBM-EGDMA).

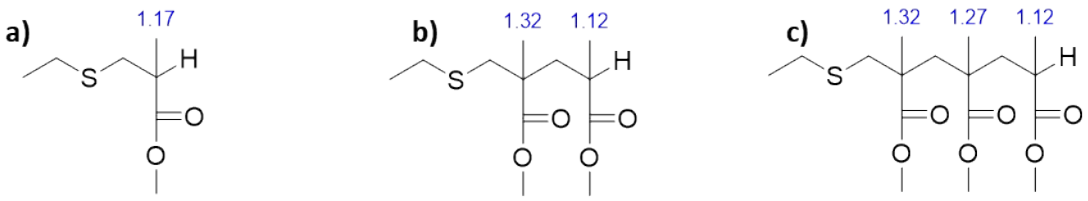


**Figure S36** Theoretical $^{1}H$ chemical shifts predicted for the methyl group protons of *poly*(MMA)-based telomers containing a) 1, b) 2 and c) 3 MMA units. These values were predicted using ChemDraw Professional – Version 18.1. These values demonstrate the impact of telomer degree of polymerisation on the chemical shift at which methyl protons resonate.

**Table S6** Traditional and modified Flory-Fox analysis of $T_g$ data obtained *via* DSC analysis of TBRT homopolymers.

| Telogen | TD-SEC | | DSC | | | Flory-Fox | Modified Flory-Fox |
|---|---|---|---|---|---|---|---|
| | $M_w$ (g mol$^{-1}$) | $M_n$ (g mol$^{-1}$) | $T_g$ (°C) | 1/ $M_n$ | 1/ ($\sqrt{M_n}.M_w$) | $Tg\infty$ (°C) ($R^2$) | $Tg\infty$ (°C) ($R^2$) |
| CHT | 59938 | 7550 | 11 | 0.00013245 | 0.00004701 | 42 (0.85) | 39 (0.94) |
| | 98528 | 10146 | 26 | 0.00009856 | 0.00003163 | | |
| | 320018 | 13304 | 31 | 0.00007517 | 0.00001533 | | |
| | 521121 | 18186 | 33 | 0.00005499 | 0.00001027 | | |
| | 4927000 | 351772 | 38 | 0.00000284 | 0.00000076 | | |
| *t*BBM | 102869 | 6204 | 15 | 0.00016119 | 0.00003958 | 45 (0.91) | 40 (1.00) |
| | 314036 | 8198 | 27 | 0.00012198 | 0.00001971 | | |
| | 638153 | 10232 | 32 | 0.00009773 | 0.00001238 | | |
| | 774323 | 20590 | 36 | 0.00004857 | 0.00000792 | | |
| | 1543000 | 25793 | 37 | 0.00003877 | 0.00000501 | | |
| PhEM | 42538 | 5948 | -8 | 0.00016812 | 0.00006287 | 19 (0.97) | 15 (0.86) |
| | 86299 | 4958 | -13 | 0.00020169 | 0.00004834 | | |
| | 135892 | 9105 | 5 | 0.00010983 | 0.00002843 | | |
| | 280461 | 11423 | 7 | 0.00008754 | 0.00001767 | | |
| | 528656 | 17793 | 9 | 0.00005620 | 0.00001031 | | |
| | 2100000 | 35343 | 14 | 0.00002829 | 0.00000367 | | |
| BzM | 116151 | 7019 | 2 | 0.00014247 | 0.00003502 | 21 (0.76) | 18 (0.91) |
| | 262407 | 9675 | 11 | 0.00010336 | 0.00001985 | | |
| | 315529 | 8765 | 6 | 0.00011409 | 0.00001902 | | |
| | 642013 | 12690 | 14 | 0.00007880 | 0.00001108 | | |
| | 2093000 | 31293 | 16 | 0.00003196 | 0.00000391 | | |

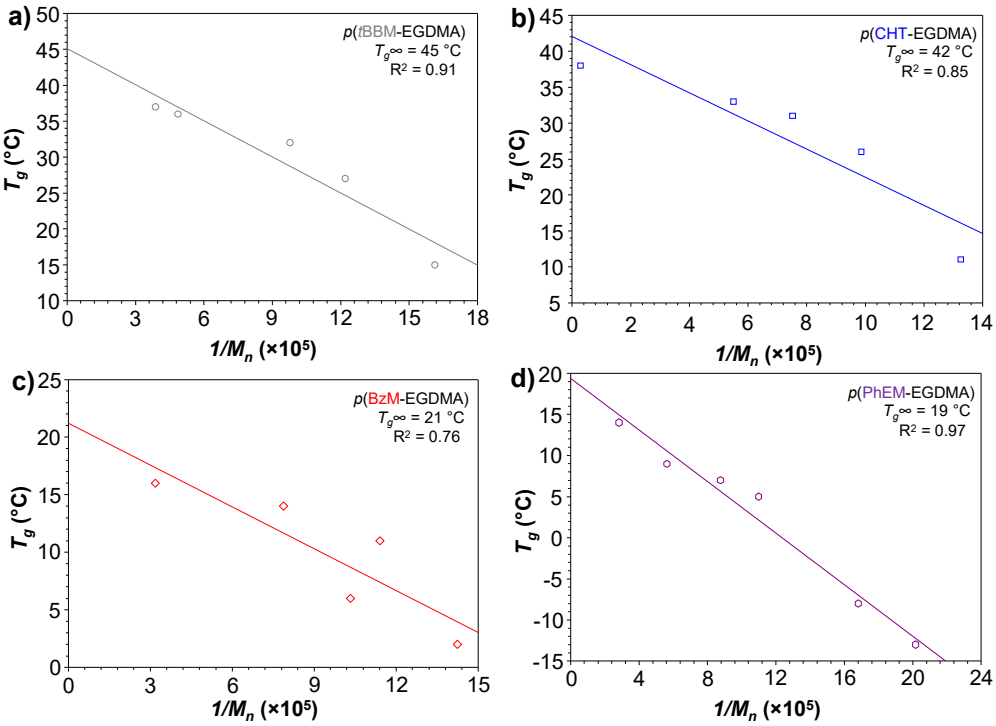


**Figure S37** Flory-Fox analysis of the thermal transitions of TBRT homopolymers. Traditional Flory-Fox plots of $T_g$ and molecular weight data obtained for a) *p*(*t*BBM-EGDMA), b) *p*(CHT-EGDMA), c) *p*(BzM-EGDMA) and d) *p*(PhEM-EGDMA).

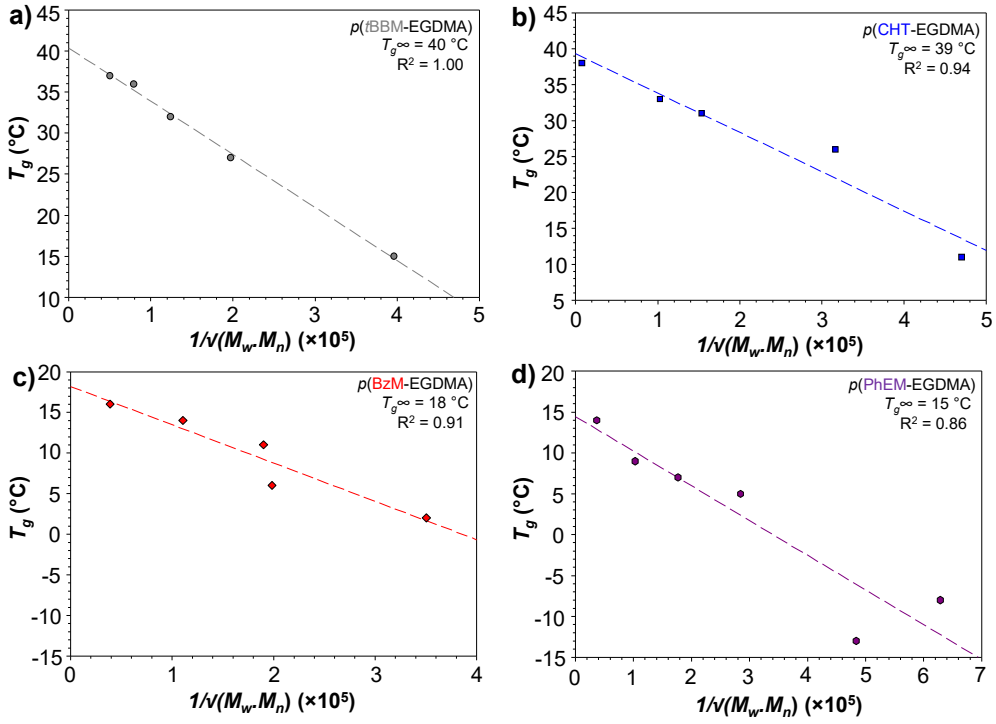


**Figure S38** Flory-Fox analysis of the thermal transitions of TBRT homopolymers. Modified Flory-Fox plots of $T_g$ and molecular weight data obtained for a) *p*(*t*BBM-EGDMA), b) *p*(CHT-EGDMA), c) *p*(BzM-EGDMA) and d) *p*(PhEM-EGDMA).